THE JOURNAL OF BIOLOGICAL CHEMISTRY VOL. 291, NO. 15, pp. 8070–8089, April 8, 2016
Published in the U.S.A.

Fibroblast Activation Protein (FAP) Accelerates Collagen Degradation and Clearance from Lungs in Mice*

Received for publication, November 12, 2015, and in revised form, December 8, 2015 Published, JBC Papers in Press, December 9, 2015, DOI 10.1074/jbc.M115.701433

Ming-Hui Fan[‡1], Qiang Zhu[§], Hui-Hua Li[‡], Hyun-Jeong Ra[¶], Sonali Majumdar[‖], Dexter L. Gulick[‡], Jacob A. Jerome[‡], Daniel H. Madsen[**], Melpo Christofidou-Solomidou[¶], David W. Speicher[‖], William W. Bachovchin[‡‡], Carol Feghali-Bostwick[§§], and Ellen Puré[¶¶]

From the [‡]Pulmonary, Allergy, and Critical Care Division, Department of Medicine, University of Pittsburgh, Pittsburgh, Pennsylvania 15213, the [§]Molecular and Cellular Pathology Graduate Program, University of North Carolina at Chapel Hill Chapel Hill, North Carolina 27599, the [¶]Department of Hematology and Oncology and the [¶¶]Departments of Biomedical Sciences and Medicine, Pulmonary Allergy and Critical Care Division, University of Pennsylvania, Philadelphia, Pennsylvania 19104, the [‖]Wistar Institute, Philadelphia, Pennsylvania 19104, the [**]Proteases and Tissue Remodeling Section, Oral and Pharyngeal Cancer Branch, NIDCR, Center for Cancer Immune Therapy, National Institutes of Health, Bethesda, Maryland 20892, the [‡‡]Sackler School of Biomedical Graduate Sciences, Tufts University, Boston, Massachusetts 02111, and the [§§]Department of Medicine, Division of Rheumatology and Immunology, Medical University of South Carolina, Charleston, South Carolina 29425

Idiopathic pulmonary fibrosis is a disease characterized by progressive, unrelenting lung scarring, with death from respiratory failure within 2–4 years unless lung transplantation is performed. New effective therapies are clearly needed. Fibroblast activation protein (FAP) is a cell surface-associated serine protease up-regulated in the lungs of patients with idiopathic pulmonary fibrosis as well as in wound healing and cancer. We postulate that FAP is not only a marker of disease but influences the development of pulmonary fibrosis after lung injury. In two different models of pulmonary fibrosis, intratracheal bleomycin instillation and thoracic irradiation, we find increased mortality and increased lung fibrosis in FAP-deficient mice compared with wild-type mice. Lung extracellular matrix analysis reveals accumulation of intermediate-sized collagen fragments in FAP-deficient mouse lungs, consistent with *in vitro* studies showing that FAP mediates ordered proteolytic processing of matrix metalloproteinase (MMP)-derived collagen cleavage products. FAP-mediated collagen processing leads to increased collagen internalization without altering expression of the endocytic collagen receptor, Endo180. Pharmacologic FAP inhibition decreases collagen internalization as expected. Conversely, restoration of FAP expression in the lungs of FAP-deficient mice decreases lung hydroxyproline content after intratracheal bleomycin to levels comparable with that of wild-type controls. Our findings indicate that FAP participates directly, in concert with MMPs, in collagen catabolism and clearance and is an important factor in resolving scar after injury and restoring lung homeostasis. Our study identifies FAP as a novel endogenous regulator of fibrosis and is the first to show FAP's protective effects in the lung.

Idiopathic pulmonary fibrosis, the most common of the idiopathic interstitial pneumonias, is characterized by inexorable progressive lung injury and scarring, with eventual death within 2–4 years from the time of diagnosis in the absence of lung transplantation (1). The etiology of the disease is poorly understood, and current Food and Drug Administration-approved treatments have only limited impact on the course of the disease (2–4).

Fibroblast activation protein (FAP,[2] also known as seprase) is a 95-kDa cell surface, type II integral serine protease belonging to the post-proline dipeptidyl aminopeptidase (DPP) family (5) that is specifically induced on lung fibroblasts in patients with idiopathic pulmonary fibrosis, in particular at the leading edge of fibrosis (6). The DPP family of serine proteases cleaves amino-terminal dipeptides from polypeptides with L-proline or L-alanine at the penultimate position. FAP is unique in that it displays additional *in vitro* endopeptidase (7), gelatinase, and potentially collagenase activity (8, 9). FAP expression is restricted, occurring at high levels on mesenchymal cells during embryogenesis (10) and then is repressed shortly after birth. In conditions associated with matrix remodeling, such as wound healing (11), fibrosis (6, 12, 13), and cancer (5, 14–17), however, FAP expression is up-regulated on activated fibroblasts. FAP has also been detected on pericytes, bone marrow-derived mesenchymal stem cells (18, 19), and a small population of macrophages (20, 21).

* This work was supported by National Institutes of Health Grants R01 CA141144 (to E. P.), R01 CA133470 (to M. C. S.), K08HL102266 (to M. H. F.), P30AR05891 (to PI Mark Gladwin; funding provided to M. H. F.), and K24 AR060297 (to C. F. B.), Dalsemer Research Award DA167003 (M. H. F.) from the American Lung Association, and in part by the Intramural Research Program of the National Institutes of Health from NIDCR (to D. H. M.), National Institutes of Health Grant R01 CA131582 (to D. W. S.), and Core Grant P30 CA010815 from NCI (to The Wistar Institute). M. C. S. has patents PCT/US14/41636 and PCT/US15/22501 pending and has a founder's equity position in LignaMed, LLC, but these have no connection to the data reported in this article. The content is solely the responsibility of the authors and does not necessarily represent the official views of the National Institutes of Health.

[1] Recipient of National Institutes of Health grants during the conduct of the study. To whom correspondence should be addressed. Tel.: 412-624-7280; Fax: 412-624-1670; E-mail: fanm@upmc.edu.

[2] The abbreviations used are: FAP, fibroblast activation protein; ECM, extracellular matrix; MMP, matrix metalloproteinase; Gy, gray; hFAP, human FAP; F, forward; R, reverse; BisTris, 2-[bis(2-hydroxyethyl)amino]-2-(hydroxymethyl)propane-1,3-diol; LAP, latency associated peptide; DPP, dipeptidyl aminopeptidase; ECD, extracellular domain; IP/IB, immunoprecipitation/immunoblotting; XRT, thoracic irradiation; MMP, matrix metalloproteinase; α-SMA, α-smooth muscle actin.

FAP's *in vivo* substrates remain unclear. Despite a lack of direct evidence, FAP is assumed to degrade ECM components, including type I collagen *in vivo* (9, 22, 23). In support of this idea, we have observed that FAP deficiency leads to increased tumor collagen content in a syngeneic transplant model of colon cancer and an endogenous K-*ras*-driven murine lung tumor model (24). In general, FAP expression by tumor stromal cells correlates with greater tumor aggressiveness, whereas inhibition of FAP activity curtails tumor growth and invasiveness (16, 24–27). Not surprisingly, cancer researchers are actively exploring FAP's therapeutic potential as a stromal cell target. In regard to fibrosis, however, FAP remains a relatively understudied protein, and its place in the pathogenesis of this disease is unknown.

The studies described herein were designed to define the role of FAP in the development of pulmonary fibrosis *in vivo*, employing a genetic approach with global knock-in mice in which the *Fap* gene has been replaced by a *lacZ* gene that is expressed under the control of the endogenous *Fap* promoter (28). Two well established complementary murine models of pulmonary fibrosis, intratracheal bleomycin and thoracic irradiation (29), were used. FAP-deficient mice demonstrated increased mortality and increased lung collagen content compared with wild-type mice in both models. This phenotype was not attributable to increased myofibroblast induction, heightened collagen synthesis, or appreciable differences in MMP activity. Instead, we present evidence that loss of FAP expression directly results in defective processing of type 1 collagen and impaired ECM remodeling. In addition, although we did not find increased numbers of α-smooth muscle actin-positive cells by immunofluorescence staining, FAP-deficient primary mouse lung fibroblasts displayed more robust induction of a myofibroblast phenotype compared with wild-type in response to TGF-β. Our findings are the first to demonstrate that FAP protects against the development of pulmonary fibrosis after lung injury.

Experimental Procedures

Animals

Eight- to 12-week-old C57BL/6 male and female mice were purchased from Charles River Laboratories. FAP-deficient $FAP^{LacZ/LacZ}$ mice (28) were obtained from W. J. Rettig and A. Schnapp (Boehringer Ingelheim Pharma KG, Ingelheim, Germany) and backcrossed 12 generations to a C57BL/6 background to facilitate fibrosis studies. These FAP-null mice have been previously characterized and show no developmental nor overt adult abnormalities under homeostatic conditions (28). Mice were genotyped as described previously (24). All mice were housed in a specific pathogen-free animal facility at the Wistar Institute or at the University of Pittsburgh. The protocols used in this study were approved by the Institutional Animal Care and Use Committee at The Wistar Institute or the University of Pittsburgh, and all procedures were conducted according to ethical committee guidelines on animal welfare and the Guide for the Care and Use of Laboratory Animals (30).

Two Murine Pulmonary Fibrosis Models

Thoracic Irradiation—Mice were anesthetized and irradiated as described previously (31). In brief, 8–12-week-old female $FAP^{LacZ/LacZ}$ mice and age/sex-matched controls were anesthetized with intraperitoneal xylazine/ketamine. A single fraction of 13.5 Gy was delivered to the thorax of the mice via a 250-kVp orthovoltage machine. A customized jig provided lead shielding over the animals' head/neck and abdomen/pelvis regions, exposing only the thorax to irradiation. Mice were followed for modified survival studies, and survivors were sacrificed 16 weeks after thoracic irradiation for tissue collection.

Intratracheal (i.t.) Bleomycin—8–12-Week-old male $FAP^{LacZ/LacZ}$ mice and age/sex-matched controls were anesthetized with intraperitoneal ketamine/xylazine. A single dose of bleomycin (1.0–1.75 IU/kg, depending on experiment) was administered by i.t. injection, using a STEPPER^{TM} repetitive pipette (Tridak^{TM}, LLC) to minimize dose variations due to pipetting error. Mice were either followed for modified survival studies or sacrificed at designated time points for tissue collection. Male mice were used as they are more bleomycin-sensitive than their female counterparts.

Hydroxyproline Assay

Collagen quantification was performed by hydroxyproline assay as previously described (24). The right lung was consistently dedicated for this assay to allow comparison. Hydroxyproline content may be converted to collagen content using the conversion factor of 1 μg of hydroxyproline corresponds to 6.94 μg of collagen.

Immunohistochemistry Staining for FAP and Immunofluorescence Staining for α-SMA

FAP Immunohistochemistry—Antigen retrieval was performed on de-paraffinized lung sections using 10 mM sodium citrate buffer, pH 6.0, for 20 min at 95 °C. Slides were washed at room temperature and hydrated in PBS. Endogenous peroxidase activity was then quenched with 3% hydrogen peroxide. Sections were then washed in PBS, 0.05% Tween 20 and endogenous avidin and biotin blocked using a commercially available avidin-biotin blocking kit (Vector Laboratories). Sections were incubated overnight at 4 °C in biotin-conjugated sheep anti-human FAP antibody (R&D Systems; AF3715; 15 μg/ml) or biotin-conjugated sheep control antibody (R&D Systems; BAF020;15 μg/ml). Sections were then washed in PBS, 0.05% Tween 20, and specific signal amplification was performed using an HRP-streptavidin/biotin-XX tyramide-containing tyramide signal amplification kit (Molecular Probes), followed by detection using the Vectastain Elite ABC kit (Vector Laboratories). $n = 3$ animals/group.

α-SMA Immunofluorescence—Immunofluorescence staining for α-SMA was performed on deparaffinized lung sections as described previously (24). Prepared slides were incubated with rabbit anti-αSMA (Abcam; ab5694; 1:100; 2 μg/ml) or isotype control antibody at 4 °C overnight. AlexaFluor-568 goat anti-rabbit IgG (Life Technologies, Inc.; A11036; 1:500) was used as the secondary antibody. Nuclei were stained with DAPI (Life Technologies Inc.; 300 nM) and mounted for fluorescence microscopy. An ImageJ macro was constructed to objectively

quantify the amount of α-SMA signal found in the total area of lung injury per field. The analysis was performed in a blinded fashion by an independent observer. For each mouse, all five lung lobes were examined, with four different ×40 images taken per lobe; $n = 3–4$ mice per group. The percentage of total injured lung area showing positive αSMA signal was quantified by computer assisted morphometry using ImageJ.

Masson Trichrome Staining

Lung sections were deparaffinized and rehydrated as described previously (24). Sections were then incubated in preheated Bouin's solution (Rowley Biochemicals) at 56 °C for 1 h. Sections were then cooled and washed in a running tap of H_2O until all yellow color was removed. Nuclei were then stained with Weigert's iron hematoxylin (Rowley Biochemicals) for 15 min. Slides were washed in a running tap of H_2O for 5 min and then rinsed with nanopure H_2O. Slides were then stained in Biebrich scarlet-acid fuchsin (Rowley Biochemicals) for 15 min, rinsed with nanopure H_2O, and then placed in phosphotungstic/phosphomolybdic acid (Rowley Biochemicals) solution for 10 min. This was followed by staining in aniline blue (Rowley Biochemicals) for 15 min. Slides were then rinsed in nanopure water, quickly dehydrated in 95 and 100% ETOH, cleared in xylene, and mounted with coverslips.

Generation of Antibody Specific for Murine FAP

Murine anti-murine FAP antibody 73.3 was produced and characterized in our laboratory as described (32). The specificity of this antibody was validated based on nonreactivity with tissues from FAP-null mice compared with analogous positive control tissues from wild-type mice.

Generation of Recombinant Murine FAP ECD

HEK293 cells transfected with murine FAP ECD containing a 5′-His and 3′-FLAG tag were obtained from Dr. Jonathan Cheng (Fox Chase Cancer Center, Philadelphia) and used to produce murine FAP ECD that was purified as described previously (32).

Immunoblotting and Murine FAP Immunoprecipitation

Immunoblotting of mouse lung homogenates and/or cell lysates was performed as described previously (24). Antibodies used were as follows: TIMP1 antibody (R&D Systems; AF980; 0.1 μg/ml); p-Smad2 (Ser-245/-250/-255) (Cell Signaling Technology; catalog no. 3104; 1:500); Smad2/3 (Cell Signaling Technology; catalog no. 5678; 1:500); α-SMA (Abcam; AB5694; 1:5000); type I collagen (EMD Millipore; AB765P; 1:500); sheep anti-human FAP (R&D Systems; AF3715; 0.5 μg/ml); β-actin (Cell Signaling Technology; catalog no. 4967; 1:1000); and GAPDH (Sigma; catalog no. G9545; 1:5000). Immunoblotting for the collagen receptor, uPARAP/Endo180, was performed on non-reduced lysates of primary mouse lung fibroblasts using a mouse monoclonal anti-Endo180 antibody generously provided by Daniel H. Madsen (33), 2 μg/ml working concentration. HRP-conjugated rabbit anti-goat, goat anti-rabbit, donkey anti-sheep, and goat anti-mouse secondary antibodies were obtained from Jackson ImmunoResearch.

Murine FAP IP/IB—Immunoblotting for detection of murine FAP was performed after immunoprecipitation. Immunoprecipitation was performed from equal amounts of protein (1 mg of lung homogenate/sample). Samples were precleared by incubating with 50 μg of isotype IgG1-conjugated agarose beads for 2 h and nutating at 4 °C. The samples were then spun down at 2000 rpm at 4 °C, and the supernatant was incubated with either 50 μg of anti-FAP 73.3-conjugated protein A-agarose beads or 50 μg of isotype IgG1-conjugated protein A-agarose beads overnight at 4 °C. The samples were then spun down at 4 °C at 2000 rpm; the supernatant was aspirated off, and the remaining beads were washed three times with 25 mM HEPES, pH 7.5, containing 0.1% Triton X-100, 300 mM NaCl, 0.5 mM DTT, 0.2 mM EDTA, 1.5 mM $MgCl_2$, containing 20 mM β-glycerophosphate, 1 mM Na_3VO_4, 10 mM NaF, 10 mM sodium pyrophosphate, and protease inhibitor mixture (Roche Applied Science) at 25 mg/ml, followed by a final PBS wash. The beads were resuspended in 2× Laemmli buffer + DTT and boiled, and 20 μl of each sample was resolved on an 8% SDS-polyacrylamide gel. The remainder of the protocol is as above, for immunoblotting, with the membranes incubated with primary anti-murine FAP 73.3 antibody overnight, followed by secondary HRP-goat anti-mouse antibody (Jackson ImmunoResearch).

Human FAP IP/IB—Immunoblotting for hFAP expression in our adenovirus experiments was performed after immunoprecipitation. Mouse lung samples were homogenized in immunoprecipitation lysis/wash buffer (Pierce) with complete mini-protease inhibitors (Roche Applied Science), and immunoprecipitation was performed with a commercial co-immunoprecipitation kit (Pierce) according to the manufacturer's instructions. Briefly, 20 μg of mouse anti-hFAP antibody (F19, Ludwig Institute for Cancer Research) and species-matched mouse IgG isotype control (MAB002, R&D Systems) were coupled and immobilized to AminoLink Plus coupling resin included in the kit. 1 mg of the mouse lung lysates were precleared with agarose-resin from the kit and then incubated (16 h; 4 °C) with antibody-bound or isotype IgG control-bound AminoLink resin. The bound protein-antibody complexes were washed with immunoprecipitation lysis/wash buffer and then eluted with the elution buffer. Samples were heated (95 °C; 5 min) and separated by two-dimensional electrophoresis on 4–12% NuPAGE® BisTris gels (Invitrogen Life Technologies, Inc.) followed by immunoblotting with sheep anti-human FAP antibody (R&D Systems; AF3715; 0.5 μg/ml) followed by HRP-conjugated donkey anti-sheep secondary antibody (Jackson ImmunoResearch, 1:5000). All immunoblots were quantified using ImageJ.

Quantitative RT-PCR

Mouse lungs were homogenized in TRIzol (Invitrogen) and processed for RNA extraction following the manufacturer's protocol. After quantification and assessment of quality/degradation by electrophoresis, reverse transcription was performed using the standard protocol for the TaqMan reverse transcription kit (Applied Biosystems). Gene expression levels were then assayed by real time PCR on an ABI Prism 7900HT real time PCR system (Applied Biosystems) using SYBR Green reagents and procedures. The results are expressed as relative gene

expression levels normalized to β-actin (gene/β-actin). Murine primer sequences are as follows: FAP-F, 5′-CACCTGATCGGCAATTTGTG; FAP-R, 5′-CCCATTCTGAAGGTCGTAGATGT; β-actin-F, 5′-TCAGCAAGCAGGAGTACGATG; β-actin-R, 5′-AACAGTCCGCCTAGAAGCACTT; αSMA-F, 5′-CCAGAGCAAGAGAGGGATCCT; αSMA-R, 5′-TGTCGTCCCAGTTGGTGATG; Col1α1-F, 5′-GCACGAGTCACACCGGAACT; Col1α1-R, 5′-AAGGGAGCCACATCGATGAT; Col1α2-F, 5′-CTACTGGTGAAACCTGCATCCA; Col1α2-R, 5′-GGGCGCGGCTGTATGAG; Col3α1-F, 5′-TCCTGAAGATGTCGTTGATGTG; Col3α1-R, 5′-TTTTTGCAGTGGTATGTAATGTTCTG; MMP2-F, 5′-ACCACCTTAACTGTTGCTTTTG; MMP2-R, 5′-AGGAAATGCAGTGGAGTGGAA; MMP3F, 5′-GGAGCTAGCAGGTTATCCTAAAAGC; MMP3-R, 5′-TAGAAATGGCAGCATCGATCTTC; MMP7-F, 5′-GGTGAGGACGCAGGAGTGAA; MMP7-R, 5′-GAAGAGTGACTCAGACCCAGA; MMP8-F, 5′-AAAAGGGAAGCTCAGTCTGTATACTC; MMP8-R, 5-AGAGGGCTGCAGAGTTAGTTACCA; MMP9-F, 5′-GGACGACGTGGGCTACGT; MMP9-R, 5′-CACGGTTGAAGCAAAGAAGGA; MMP13-F, 5′-TTGCCCTGGGAAGGAGAGA; MMP13-R, 5′-AGTCCAGCTCAACAAGAAGAAGGT; MMP14(MT1-MMP)-F, 5′-AGTCAGGGTCACCCACAAAGA; MMP14 (MT1-MMP)-R, 5′-TTTGGGCTTATCTGGGACAGA; PAI-1-F, 5′-TTGTCCAGCGGGACCTAGAG; PAI-1-R, 5′-AAGTCCACCTGTTTCACCATAGTCT; CTGF-F, 5′-CACTCTGCCAGTGGAGTTCA; CTGF-R, 5′-AAGATGTCATTGTCCCCAGG; TIMP1-F, 5′-CCTTCGCATGGACATTATTCTC; and TIMP1-R,5′-TCTCTAGGAGCCCCGATCTG. In our later adenovirus experiments, we used TaqMan methodology; mouse lung tissues were homogenized by metal-probe homogenizer and total RNA isolated by RNeasy mini kit (Qiagen). 1 μg of total RNA was reverse-transcribed into cDNA using the high capacity cDNA reverse transcription kit (Applied Biosystems). Quantitative real time PCR was performed using the TaqMan gene expression assay on an Applied Biosystems 7900HT fast real time PCR system according to the manufacturer's instructions. TaqMan gene expression master mix (Applied Biosystems) and commercially designed human FAP (catalog no. 4331182 ID:Hs00990806_m1) and 18S (catalog no. 4333760F, for detection in mouse, rat, and human) primer/probe sets were purchased from Applied Biosystems. ΔCT $Ct(\text{FAP}) - Ct(18\text{S})$ was used to represent the expression level of human FAP in the mouse lung after adenovirus administration.

Gelatin Zymography

Mouse lungs were homogenized in MPER buffer (Pierce) in the presence of protease inhibitor mixture without EDTA (Roche Applied Science). Protein concentration was determined by BCA assay (Pierce), and 20 μg of each lung homogenate were mixed with 2× non-reducing sample buffer containing 2% SDS, 0.1% bromphenol blue, and 40% glycerol. The samples were incubated at room temperature for 30 min and then loaded onto 8% SDS-polyacrylamide gels containing 0.5 mg/ml gelatin (Sigma). After electrophoresis, the gels were washed four times at room temperature for 15 min with 2.5% Triton X-100 solution and then incubated overnight in activation buffer containing 50 mM Tris-HCl, 200 mM NaCl, 5 μM $ZnCl_2$, 5 mM $CaCl_2$, and 0.02% NaN_3, pH 7.5, for 18 h at 37 °C. The gels were then stained with 0.125% Coomassie Blue in 60% methanol and 25% acetic acid for 1 h at room temperature followed by destaining in 10% acetic acid with 30% methanol until bands appeared.

Collagen Zymography

Collagenase activity in lung homogenates was assessed by collagen zymography as described in the literature (34). In brief, lungs were homogenized in MPER buffer (Pierce) in the presence of protease inhibitor mixture without EDTA (Roche Applied Science). Protein concentration was determined by BCA assay (Pierce) and 50 μg of lung homogenate mixed with 4× non-reducing sample buffer containing 200 mM Tris-HCl, pH 6.8, 8% SDS, 0.4% bromphenol blue, and 50% glycerol. The samples were then incubated at room temperature for 10 min and loaded onto 8% SDS-polyacrylamide gels containing 0.5 mg/ml rat tail type 1 collagen (BD Biosciences). After electrophoresis, the gels were washed twice for 1 h at room temperature with 2.5% Triton X-100 solution and then incubated in activation buffer containing 100 mM Tris, 5 mM $CaCl_2$, 150 mM NaCl, 0.01% Brij-35 at pH 8.0 for 40 h at 37 °C. The gels were then stained with 0.25% Brilliant Blue R-250 in 40% methanol and 10% acetic acid solution for 2 h at room temperature. The gels were then destained in aqueous 10% methanol and 10% acetic acid solution until the bands appeared.

Collagen Digests

Gels containing 2 mg/ml rat tail type 1 collagen (BD Biosciences) in PBS were made, using 0.1 M NaOH to neutralize the collagen pH and incubated at 37 °C for 1 h to promote solidification (22). For each 45 μg of collagen (*i.e.* 22.5 μl of gel), 0.75 μg of recombinant human MMP-1 (R&D Systems) in 12.5 mM sodium phosphate was added, and the mixture was incubated for 8 h at 37 °C. GM6001 (50 μM) was then added, and the sample was incubated for 15 min at 37 °C to ensure inhibition of further MMP activity. Recombinant murine FAP ECD was then added in increasing amounts (0.25–5 μg) to generate a dose-response curve. In an additional sample, FAP-ECD (5 μg) pre-incubated for 15 min at 37 °C with PT630 (50 μM, Point Therapeutics, Inc.), a pharmacologic inhibitor of both FAP and dipeptidyl peptidase IV (DPPIV), rather than FAP-ECD alone, was added to the sample to verify specificity of the assay. After an 8-h incubation at 37 °C with FAP ECD ± inhibitor, the collagen digests were prepared for electrophoresis by adding 4× sample buffer and reducing agent and heating at 70 °C for 10 min. Equal volumes of the collagen digests were separated by two-dimensional electrophoresis on a 4–12% Bis-Tris gel (Invitrogen) with MES running buffer. A small aliquot of undigested, acid-solubilized type 1 rat tail collagen was also included as a reference for intact type I collagen. The soluble fraction of a collagen gel exposed only to FAP ECD for 8 h at 37 °C (*i.e.* no prior digestion with MMP-1) was also included. The gel was then stained with SimplyBlue™ SafeStain Coomassie G-250 stain (Invitrogen), destained in nanopure water, and photographed.

FAP/TGF-β Cleavage Experiments

Recombinant murine FAP (R&D Systems) was purchased for these experiments. Enzymatic activity of the protein was confirmed by sequential type I collagen digests (*i.e.* MMP1 followed by recombinant murine FAP) as outlined above prior to proceeding with our TGF-β experiments. Recombinant proteins tested as potential candidates for FAP-mediated proteolytic cleavage were as follows: active recombinant human TGF-β (R&D Systems), recombinant latent human TGF-β (LTGF-β, Cell Signaling Technology), and recombinant human latency-associated peptide (R&D Systems). 1 μg of each protein was incubated either alone, together with 2.5 μg of recombinant murine FAP, or with 2.5 μg of FAP preincubated with the FAP inhibitor, *N*-(quinoline-4-carbonyl)-Gly-Pro(*F,F*)-nitrile, 2 mM, at 15 min for 16 h at 37 °C in 25 mM Tris-HCl, 0.25 M NaCl, pH 8.0, and a total sample volume of 25 μl. Samples were then resolved on a 4–12% Bis-Tris gel (Invitrogen) with MES running buffer, stained for protein using the SilverQuest™ silver staining kit (ThermoFisher Scientific), per the manufacturer's instructions, and photographed.

Lung ECM Isolation and Detection of Collagen Fragments

Lung ECM was isolated from the lungs of mice 10 days after i.t. bleomycin *versus* saline injection using a modification of a protocol for ECM isolation from murine left ventricles (35–37). Lungs were washed in wash buffer (nanopure water plus 20 mM EDTA and complete protease inhibitor mixture (Roche Applied Science)) for 30 min on a rocker at room temperature. Lungs were then decellularized over a 72–96-h period and rocking at room temperature, using several changes of decellularization buffer (1% SDS with complete protease inhibitor mixture and 20 mM EDTA in PBS). Lungs were then washed in wash buffer for 5 min three times, then overnight, rocking at room temperature Lungs were then snap-frozen, pulverized, then homogenized, and sonicated in Protein Extraction Reagent IV (Sigma) with 1× complete protease inhibitor mixture. Protein concentration was determined by Bradford assay. 0.75 μg of each ECM preparation was resolved by two-dimensional electrophoresis using 3–8% Tris acetate gels (Invitrogen) to better separate intact collagen forms, and 2.0 μg of each ECM preparation was simultaneously resolved on 4–12% Bis-Tris gels, to better separate out and detect smaller sized collagen fragments. Standard protocol for immunoblotting was performed with the exception that the PVDF membranes were cut roughly halfway between the 150- and 100-kDa markers to allow the two halves of the membrane to be incubated in primary antibody separately. This prevented the primary antibody from being consumed and bound preferentially to the much more abundant intact collagen forms in our preparations, allowing better detection of the intermediate-sized collagen fragments on the lower portion of the PVDF membrane. Polyclonal rabbit anti-mouse type 1 collagen antibody (Millipore) was used as the primary antibody, followed by HRP-conjugated goat anti-rabbit secondary antibody (Jackson ImmunoResearch). Experiments were repeated in triplicate for a total of $n = 3$ per group.

Primary Mouse Lung Fibroblast Culture Experiments

Primary mouse lung fibroblasts were isolated and cultured as described previously (38). All experiments involving primary lung fibroblasts were performed three times with cells at P3-P4, using different animals for isolation of cells for each experiment. Primary mouse lung fibroblasts were plated at a density of 2×10^5 cells/well on type 1 collagen-coated 6-well plates. The exception to this were experiments to detect collagen fragments in cell culture media; here, cells were plated on plastic. Recombinant human TGF-β (R&D Systems) stimulation was performed at 10 ng/ml. p-Smad2 and Smad 2/3 levels were evaluated after 90 min of recombinant human TGF-β exposure. α-SMA protein expression was assessed at 48 h (Fig. 8*C*) and 72 h (data not shown) of TGF-β exposure. Detection of type 1 collagen fragments in cell culture media was performed at 72 h of TGF-β exposure.

Collagen Internalization Experiments

Type I rat tail collagen (BD Biosciences) was labeled with DyLight 650 (Pierce) as described previously (39). The dye concentration was adjusted to achieve 1 dye molecule per 3–5 collagen triple helix labeling efficiency. The unreacted dye was removed by serial collagen precipitations with 0.9 M NaCl in 0.5 M acetic acid. Purified collagen was solubilized in 2 mM HCl, characterized by electrophoresis on pre-cast 3–8% Tris acetate mini-gels (Invitrogen), and collagen concentration was determined by circular dichroism in a J810 spectrometer (Jasco) using known dilutions of unlabeled type I rat tail collagen (BD Biosciences) to generate a standard curve. Gels containing 400 μg/ml DL650-labeled collagen were made in 12-well tissue culture plates and allowed to dry overnight. The following day, the gels were washed with sterile water to remove excess salts and equilibrated with 1× PBS followed by DMEM washes. Mouse lung fibroblasts from wild-type or $FAP^{LacZ/LacZ}$ mice were pretreated with 20 μM E-64d (Sigma), a lysosomal inhibitor that prevents lysosomal degradation of internalized collagen, for 1 h, then seeded at 1.4×10^5 cells/well on the collagen gels, and incubated at 37 °C for 9 h in the continued presence of E-64d. Fibroblasts were similarly plated on unlabeled collagen gels to serve as appropriate negative controls. Cells were then recovered from the gels, and surface-bound collagen was removed via a collagenase IV (Sigma) digestion followed by trypsin to achieve a single-cell suspension. Cells were then plated on fibronectin-coated glass coverslips and incubated overnight in the presence of E-64d. Cells were then fixed with 3.75% paraformaldehyde and stained with Hoechst dye for nuclei and AF488-labeled F-actin antibody. Confocal microscopy was conducted using an Olympus Fluoview 1000 confocal microscope to obtain 15–18 images from five coverslips per group. Quantitation of the integrated DL650 fluorescence per image was performed using Metamorph software, and this value was divided by the nuclei per high power field to calculate DL650 fluorescence/cell for each image. Imaging of fibroblasts seeded on unlabeled collagen gels confirmed the absence of virtually any detectable autofluorescence in the DL650 channel in our controls. Experiments were performed in triplicate. The collagen internalization experiments above were also repeated in the

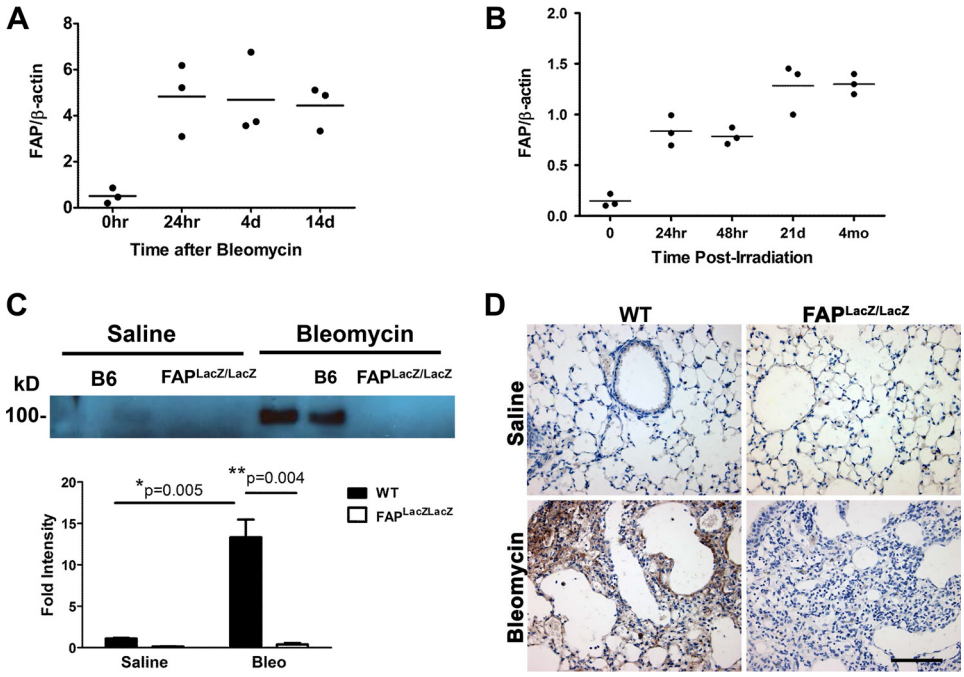

FIGURE 1. **Rapid and sustained increase in FAP expression following bleomycin and XRT-induced lung injury.** Kinetics of FAP mRNA induction in the lungs of male C57BL/6 mice after a single dose of i.t. bleomycin (1.75 IU/kg) (*A*) and in the lungs of female C57BL/6 mice after a single dose of 13.5 Gy thoracic irradiation (*B*). FAP mRNA expression is normalized to β-actin. In both models, FAP gene expression was undetectable in the lungs of $FAP^{LacZ/LacZ}$ mice at all time points. *C,* representative FAP IP/IB confirming induction of FAP at the protein level in wild-type C57BL/6 mouse lungs 7 days after i.t. bleomycin (*top*). Densitometry of the FAP IP/IB bands by Image J (*bottom*), $n = 4$ per group. *D,* immunohistochemistry staining for FAP on paraffin-embedded lung sections from mice 14 days after i.t. bleomycin *versus* saline. ×40, *scale bar,* 100 μm.

presence or absence of a selective FAP inhibitor, *N*-(quinoline-4-carbonyl)-Gly-Pro(*F,F*)-nitrile. FAP^{+} primary mouse fibroblasts derived from wild-type mice were preincubated with either vehicle control or *N*-(quinoline-4-carbonyl)-Gly-Pro(*F,F*)-nitrile at 1 mM concentration in cell culture media for 1 h. The cells were then seeded on DL650-labeled collagen gels, and the experiments were carried forward exactly as outlined previously except that the cells were also maintained in FAP inhibitor *versus* vehicle control in addition to the lysosomal inhibitor, E-64d, for the duration of the experiment. Quantification of DL650 fluorescence/cell was performed using NIS Elements on 15–16 images per condition, using fixed settings and with the binary threshold set so that there was no significant signal seen on negative control images of cells seeded on unlabeled collagen gels.

Adenoviral Reconstitution of FAP Expression

The full-length human *FAP* gene sequence was cloned into the shuttle plasmid, pAdlox, and adenoviruses expressing hFAP (adeno-hFAP) and empty vector (adeno-Y5) were made and purified with assistance from the Vector Core Facility at the University of Pittsburgh. FAP-null and wild-type primary mouse lung fibroblasts were then transduced with adeno-hFAP and adeno-Y5. We confirmed robust FAP expression by both IPIB and FACS (data not shown). Proceeding to *in vivo* experiments, 10^8 pfu of adeno-hFAP *versus* adeno-Y5 were administered by i.t. injection in 40 μl of sterile PBS to 8–12-week-old male $FAP^{LacZ/LacZ}$ mice and age/sex-matched C57BL/6 controls. 72 h later, 1.0 IU/kg i.t. bleomycin was administered in 40 μl of sterile normal saline to each mouse ($n = 6–10$/group, four groups total). Mice were later sacrificed at 15 days post-bleomycin for hydroxyproline assay (R lung) and histological analysis (L lung). Another experiment was conducted with mice treated with 10^8 pfu of adeno-hFAP *versus* adeno-Y5 alone with animals sacrificed at various intervals to examine the changing kinetics of hFAP gene and protein expression over time.

Statistics

All results are expressed as mean ± S.E. Statistical analysis was performed using one-way analysis of variance with the Tukey's multiple comparison test and two-tailed Student's *t* test (Prism 5.0, GraphPad Software). Statistical significance of survival curves was assessed using the log-rank test. *p* values of less than 0.05 were considered statistically significant. Western blots were quantified using ImageJ software and analyzed for relative density of bands.

Results

Wild-type Mice Demonstrate Rapid and Sustained Up-regulation of FAP Expression in Two Murine Models of Pulmonary Fibrosis—We verified that FAP is induced in two separate pulmonary fibrosis models. Rapid and sustained induction of *Fap* gene transcription occurred within 24 h of i.t. bleomycin administration in C57BL/6 wild-type mice by RT-PCR (Fig. 1*A*). *Fap* mRNA levels remained high even 14 days after injury (Fig. 1*A*). Similarly, *Fap* gene expression was up-regulated by 24 h after thoracic irradiation (XRT) and remained elevated 4 months later, the latest time point analyzed (Fig. 1*B*). *Fap* gene expression was undetectable in the lungs of $FAP^{LacZ/LacZ}$ mice at all time points. Up-regulation of FAP expression in wild-type mice after bleomycin was confirmed by IP/IB of whole lung

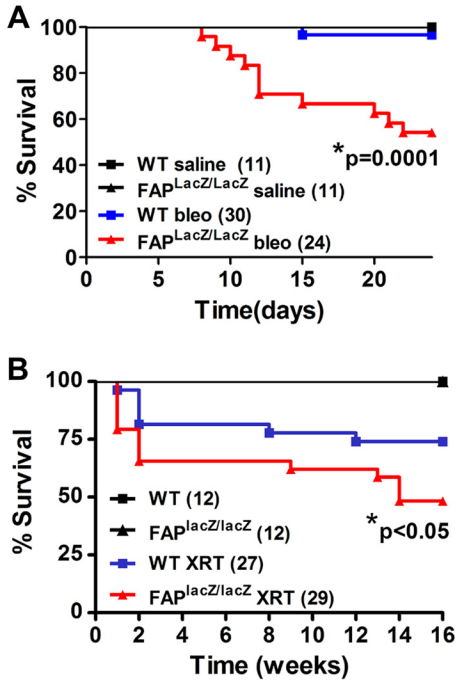

FIGURE 2. **Decreased survival of FAP-deficient mice following bleomycin and XRT-induced lung injury.** *A,* decreased survival in male FAP-null $FAP^{LacZ/LacZ}$ mice *versus* wild-type controls after a single dose of i.t. bleomycin (*bleo*) (1.0 IU/kg), * indicates $p < 0.01$. Mice were followed for 24 days after treatment. There were also statistically significant differences in survival between saline *versus* bleomycin-treated mice in each genotype, $p < 0.01$. *B,* decreased survival in female FAP-null $FAP^{LacZ/LacZ}$ mice *versus* wild-type controls after a single dose of 13.5 Gy thoracic irradiation, * indicates $p < 0.05$. Mice were followed for 16 weeks after treatment. There were also significant differences in survival between untreated *versus* thoracic-irradiated mice in each genotype, $p < 0.01$. The number of animals per group is indicated in *parentheses*.

homogenates (Fig. 1*C*) and also by immunohistochemistry (Fig. 1*D*). Tissue staining (Fig. 1*D*) demonstrates FAP expression predominantly on stromal cells rather than on the inflammatory infiltrate or alveolar epithelial cells.

FAP-deficient Mice Show Decreased Survival Compared with Wild-type Controls in Two Murine Models of Pulmonary Fibrosis—FAP-deficient $FAP^{LacZ/LacZ}$ mice and age/sex-matched wild-type controls received 1.0 IU/kg i.t. bleomycin *versus* saline control or a single dose of 13.5 Gy thoracic irradiation *versus* no treatment and were followed for survival. In the bleomycin model, there was minimal mortality in the wild-type at the 1.0 IU/kg dose but 50% mortality in the $FAP^{LacZ/LacZ}$ mice (Fig. 2*A*). $FAP^{LacZ/LacZ}$ mice had roughly 50% mortality at 16 weeks after thoracic XRT compared with 25% in wild-type controls (Fig. 2*B*).

FAP-deficient Mice Demonstrate Increased Lung Collagen Content and Pulmonary Fibrosis Compared with Wild-type Controls in Two Murine Models of Pulmonary Fibrosis—To evaluate whether the increased mortality in FAP-deficient mice was caused by increased lung fibrosis, we assessed the lung collagen content in both pulmonary fibrosis models by two independent methods as follows: 1) trichrome stain (Fig. 3, *A* and *B*), and 2) a quantitative hydroxyproline assay (Fig. 3, *C* and *D*). Trichrome staining suggested greater lung collagen content following injury in FAP-null $FAP^{LacZ/LacZ}$ mice compared with wild-type mice in both models. Quantification of lung collagen content by hydroxyproline assay confirmed this. Interestingly, untreated $FAP^{LacZ/LacZ}$ mice demonstrated a small but statistically significant increase in lung hydroxyproline content at the 16-week time point compared with untreated wild-type controls (Fig. 3*D*). Similar to humans, mice develop a mild degree of interstitial thickening and lung scarring with normal aging. Although not apparent in early adulthood (see saline-treated animals, 10–14 weeks old, Fig. 3*C*), FAP-deficient mice experience a slight acceleration in the gradual increase in lung collagen content and fibrosis associated with aging, a finding demonstrable at 24–28 weeks of age (see Fig. 3*D*, *untreated*).

There Is No Apparent Difference in the Myofibroblast Population in FAP-deficient and Wild-type Mice to Account for the Difference in Phenotype—In recent years, the α-SMA^+ myofibroblast has commanded the attention of researchers in the fibrosis field. With its enhanced contractile properties and exuberant matrix production, the myofibroblast has been highlighted as a key player in fibrogenesis (40–42). We therefore investigated whether increased myofibroblast numbers in the FAP-null mice compared with wild-type could be responsible for the observed phenotype. Whole lung α-SMA mRNA levels were determined by RT-PCR in both fibrosis models (Fig. 4, *A* and *B*), 7 days post-i.t. administration of bleomycin *versus* saline and 16 weeks post-13.5Gy thoracic XRT *versus* no treatment. Although α-SMA expression was induced by bleomycin exposure, there were no significant differences between FAP-null and wild-type control mice within treatment groups (Fig. 4*A*). In the XRT model, there appeared to be minimal induction of myofibroblasts (Fig. 4*B*); in fact, lung α-SMA transcript levels in treated mice trended lower than those in controls. Lung α-SMA immunofluorescence staining (Fig. 4, *C* and *D*) was performed to confirm these mRNA findings. This was performed at 14 days post-i.t. administration of bleomycin *versus* saline and 16 weeks post-13.5 Gy thoracic radiation *versus* no treatment. Objective quantification of percent α-SMA staining per total injured lung area revealed no differences between FAP-deficient $FAP^{LacZ/LacZ}$ mice and wild-type mice after either i.t. bleomycin or thoracic irradiation exposure (Fig. 4, *E* and *F*). The FAP-null phenotype therefore did not appear to be driven by differential induction of the α-SMA^+ myofibroblast population.

Increased Lung Fibrosis and Mortality in the FAP-null Mice Cannot Be Attributed to Differences in MMP Activity or Known Profibrotic Factors or Increased Collagen Synthesis—Gene expression levels of multiple *MMPs*, *Timp1*, *Pai-1*, and *Ctgf* (known players in fibrosis and collagen catabolism and turnover) were also assessed (Fig. 5). We found no significant differences between bleomycin-treated FAP-null and wild-type mice, although in the XRT model, there was a significant decrease in *Timp1* and *Pai-1* transcript levels in the irradiated FAP-null mice compared with wild type. Gelatin and collagen zymography performed on whole lung lysates 10 days after bleomycin administration revealed no discernable differences in overall MMP enzymatic activity (Fig. 6). We assessed TIMP1 protein levels in the bleomycin model to see if differential TIMP1 expression could be modulating MMP activity. Although bleomycin induced TIMP1 expression, there was no

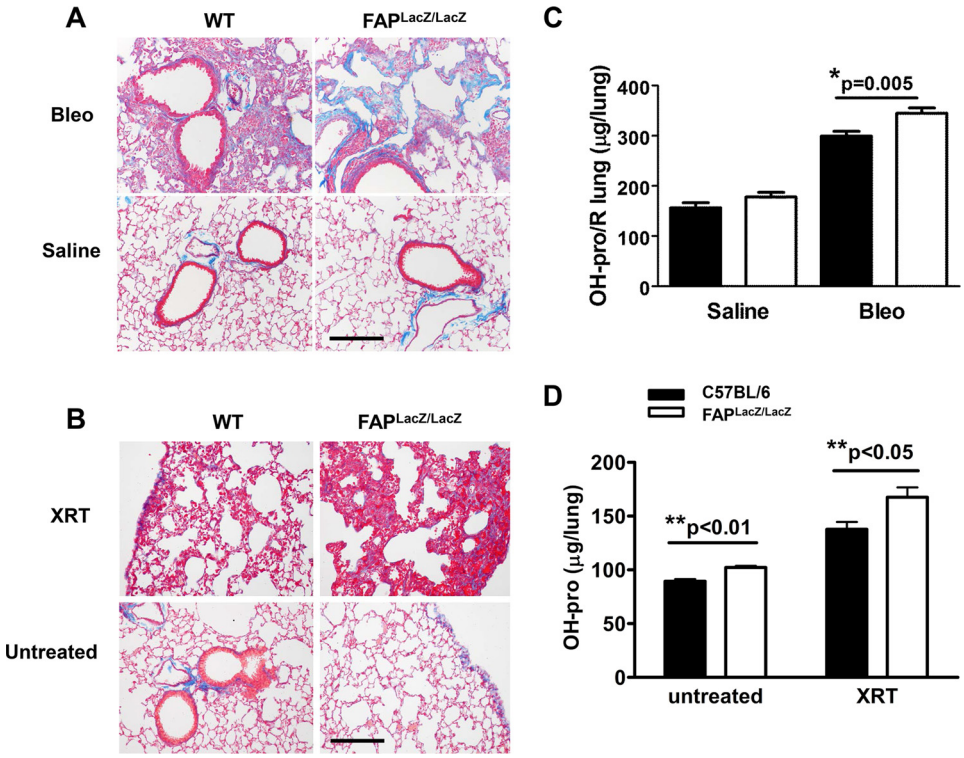

FIGURE 3. **Excess accumulation of collagen in FAP-deficient mice following bleomycin and XRT-induced lung injury.** *A,* representative trichrome staining of lungs from FAP-deficient FAP$^{LacZ/LacZ}$ *versus* wild-type mice 14 days after i.t. bleomycin (*Bleo*) (1.75 IU/kg) *versus* saline, ×20, *scale bar,* 200 μm. *B,* representative trichrome staining of lungs from FAP-deficient FAP$^{LacZ/LacZ}$ *versus* wild-type mice 16 weeks after 13.5 Gy thoracic irradiation *versus* no treatment, ×20, *scale bar,* 200 μm. *C,* quantification of total right lung collagen content by hydroxyproline assay 14 days after i.t. bleomycin (1.0 IU/kg) administration, $n = 5–10$ mice per group. There was a significant increase in lung hydroxyproline content between saline- and bleomycin-treated mice for each genotype, $p < 0.01$. *D,* quantification of right lung collagen content by hydroxyproline assay 16 weeks after 13.5 Gy thoracic irradiation *versus* no treatment, $n = 4–8$ mice per group. There was also a significant increase in lung hydroxyproline content between untreated and thoracic-irradiated mice in each genotype, $p < 0.01$.

significant difference in TIMP1 levels in bleomycin-treated FAP-null FAP$^{LacZ/LacZ}$ *versus* bleomycin-treated wild-type mouse lungs (Fig. 7).

FAP-deficient Primary Mouse Lung Fibroblasts Display More Robust Induction of the Myofibroblast Phenotype by TGF-β Compared with Wild Type—It is well accepted that TGF-β plays a pivotal role in the development of fibrosis. Produced by multiple cell types, including T cells, macrophages, neutrophils, and fibroblasts, it is perhaps the most well known and potent pro-fibrotic cytokine, functioning in some ways like a master switch (43). We looked for evidence of enhanced TGF-β activation in FAP-null FAP$^{LacZ/LacZ}$ mice by evaluating phospho-Smad2 levels in whole lung homogenates in the bleomycin model. Although there was a significant increase in phospho-Smad2 levels between saline- and bleomycin-treated animals, there was no significant difference in phospho-Smad2 levels between the two genotypes within either treatment group (Fig. 8*A*). We also assessed TGF-β production in FAP-deficient FAP$^{LacZ/LacZ}$ *versus* wild-type primary mouse lung fibroblasts in response to wounding using a mink luciferase epithelial cell reporter assay and found no differences between cell types (data not shown).

Although there was little evidence that altered TGF-β signaling was responsible for the observed FAP-null phenotype at the tissue level (Fig. 8*A*), this likely was due to the fact that the multiple cell types present drowned out any fibroblast-specific signal. We therefore proceeded to examine more cell type-specific responses and explored the effect of TGF-β exposure on primary mouse lung fibroblasts isolated from the lungs of FAP$^{LacZ/LacZ}$ *versus* wild-type mice. This revealed a heightened increase in phospho-Smad2 levels at 90 min (Fig. 8*B*) and induction of α-SMA at 48 h (Fig. 8*C*) and 72 h (data not shown) in FAP-deficient primary mouse lung fibroblasts *versus* wild type in response to TGF-β stimulation. In addition, soluble fragments of type I collagen in cell culture media were increased in FAP-deficient primary mouse lung fibroblasts after 72 h of TGF-β exposure compared with wild type (Fig. 8*D*). This most likely reflects both increased type I collagen synthesis in the presence of TGF-β and decreased breakdown of intermediate-sized collagen fragments in the absence of FAP. To support this hypothesis, FAP-deficient primary mouse lung fibroblasts display increased α-SMA levels and increased amounts of soluble type I collagen in cell culture media at baseline, prior to TGF-β stimulation (see *CON* in Fig. 8, *C* and *D*). We assessed TGFβ receptor 1 and 2 levels as well as levels of the inhibitory Smad6 and -7, but we found no differences that could account for the observed differences in TGF-β responses between the two fibroblast cell types (data not shown). We then explored whether FAP could cleave and thereby activate or inactivate TGF-β (Fig. 8*E*). FAP did not cleave either active or inactive TGF-β to any significant degree. Examination of the protein sequence of TGF-β did reveal a possible PPGP cleavage site in the LAP. Incubation of recombinant murine FAP with recombinant human LAP did generate two faint new smaller

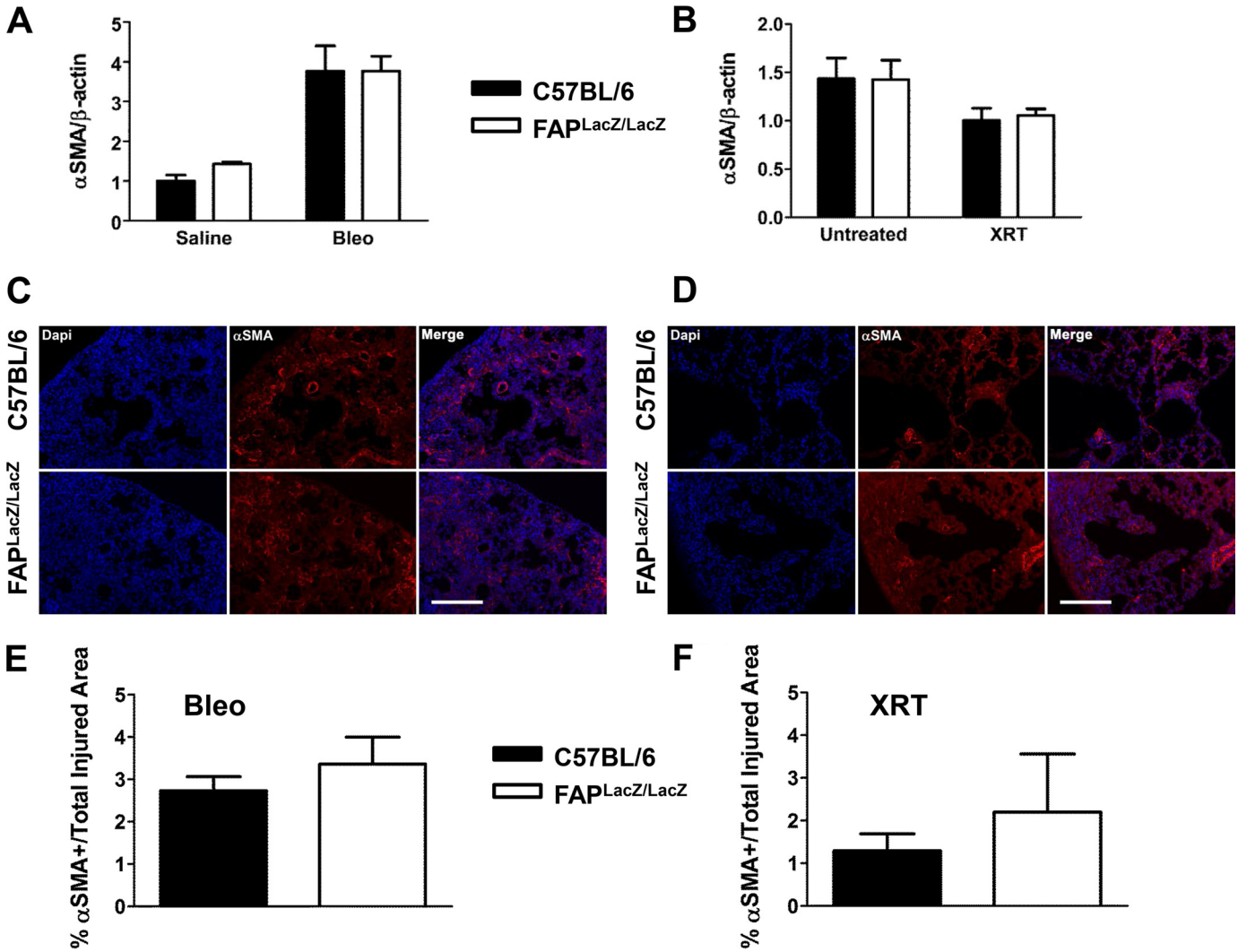

FIGURE 4. **FAP does not regulate α-SMA expression following lung injury.** *A,* α-SMA mRNA levels were higher 7 days after i.t bleomycin (*Bleo*) in both wild-type and $FAP^{LacZ/LacZ}$ mice compared with controls by RT-PCR, but there was no significant difference in α-SMA transcript levels between the two genotypes when comparing within treatment groups. α-SMA mRNA expression is normalized to β-actin. $n = 3$/group. *B,* trend toward a decrease in α-SMA mRNA expression in mice of both genotypes by RT-PCR 16 weeks after 13.5 Gy thoracic irradiation compared with no treatment, but these differences were not statistically significant. α-SMA mRNA expression is normalized to β-actin. $n = 3–5$/group. *C,* representative α-SMA immunofluorescence staining of lungs from $FAP^{LacZ/LacZ}$ and wild-type mice 14 days after i.t bleomycin. Sections from saline-treated animals are not shown as they had virtually no fibroblast-associated α-SMA staining. ×20, *scale bar,* 200 μm. $n = 4$/group. *D,* representative α-SMA immunofluorescence staining of lungs from $FAP^{LacZ/LacZ}$ and wild-type mice 16 weeks after 13.5 Gy thoracic irradiation. Sections from untreated animals are not shown as they had virtually no fibroblast-associated α-SMA staining. ×20, *scale bar,* 200 μm. $n = 4$/group. *E,* quantification of α-SMA staining in the bleomycin-treated mice by ImageJ. All five lung lobes from each mouse were examined with four ×40 images taken per lobe and analyzed in blinded fashion by an ImageJ macro designed to quantify the area positive for α-SMA staining within areas of lung injury. Total area positive for α-SMA immunofluorescence was divided by total injured area for each mouse. $n = 4$/group. *F,* quantification of α-SMA staining in the irradiated mice by ImageJ in the same manner as described in *E*. $n = 3–4$/group.

protein bands, indicating a modest degree of LAP cleavage by FAP (indicated by *arrows* in Fig. 8*E*). These bands disappeared when FAP was preincubated with the FAP inhibitor, showing specificity of the result. The significance of this finding, however, is unclear.

We investigated whether FAP-null mice might produce more collagen in response to lung injury than wild-type mice. mRNA levels of several major collagen isoforms found in the lung (*i.e.* collagen 1α1, 1α2, and 3α1) were significantly upregulated following injury in both pulmonary fibrosis models (Fig. 9*A*). However, no significant differences in lung transcript levels of these collagen isoforms were found between the two genotypes after bleomycin treatment. In the XRT model, irradiated FAP-null mice actually had lower mRNA levels of these collagen isoforms compared with their irradiated wild-type counterparts, perhaps due to a negative feedback mechanism.

FAP Participates in Type 1 Collagen Catabolism after Prior MMP-mediated Cleavage of Intact Collagen to Its ¾- and ¼-Length Fragments—The data above revealed increased collagen accumulation in FAP-null mice compared with controls in the absence of evidence for increased collagen synthesis or alterations in other proteases/factors typically associated with collagen turnover. We therefore postulated that FAP itself plays an essential role in collagen proteolysis and ECM remodeling so that absence of FAP activity leads to impaired collagen break-

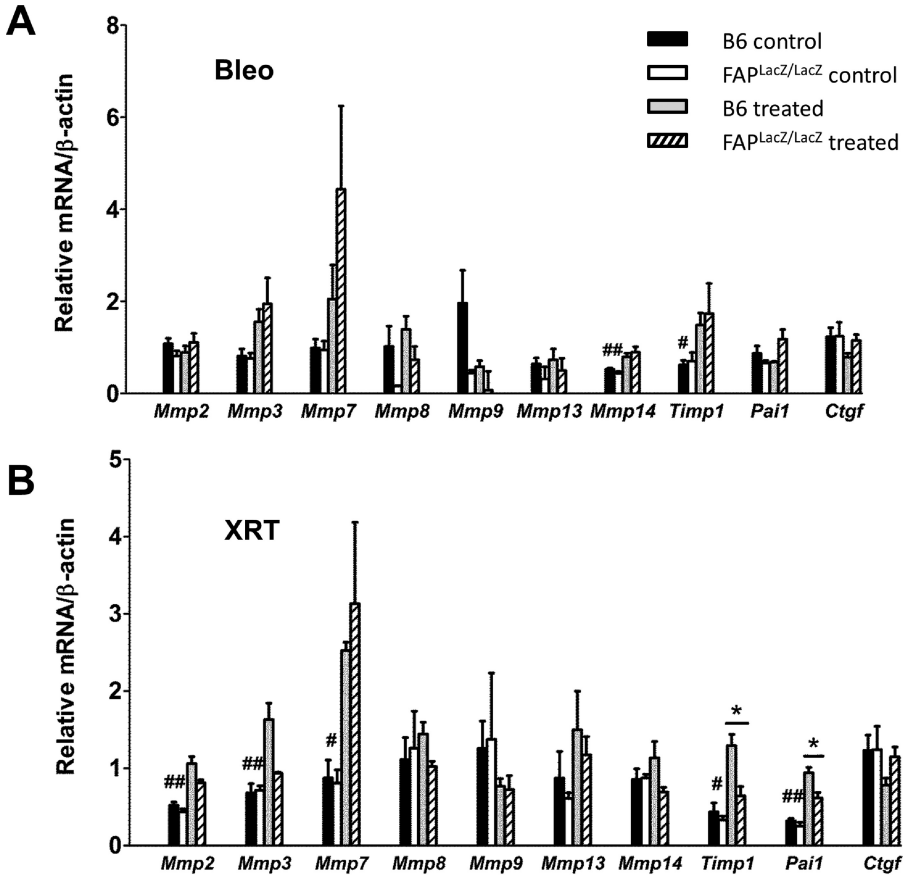

FIGURE 5. **Levels of MMPs and several other known pro-fibrotic factors are similar in the lungs of FAP$^{LacZ/LacZ}$ and wild-type mice after i.t. bleomycin or thoracic irradiation.** *A,* lung mRNA levels of multiple MMPs and several known profibrotic factors were measured by RT-PCR in mice 7 days after i.t. bleomycin (*Bleo*) (1.75 IU/kg) *versus* saline (*A*) and 16 weeks after thoracic irradiation (13.5 Gy) *versus* untreated (*B*). $n = 3$ mice per group, mRNA levels were normalized to β-actin. # indicates a significant difference between wild-type control and wild-type treated mice, $p < 0.05$. ## indicates a significant difference between control and treated mice for both genotypes, $p < 0.05$. * indicates a significant difference between XRT-treated FAP$^{LacZ/LacZ}$ and XRT-treated wild-type mice, $p < 0.05$.

down and clearance after lung injury. We analyzed the sequence of type I collagen for defined consensus FAP target sequences (endopeptidase, DGESGP and DRGETGP; DPP, PPGP) and found innumerable potential DPP cleavage sites for FAP along the length of the 1α1 chain of the type I collagen fibril (data not shown). Analogous sites were also mapped to the 1α2 chain of type I collagen and the 3α1 chain of type III collagen (data not shown).

In vitro studies sought to confirm a reported lack of FAP collagenase activity (Fig. 9*B*) (22). Incubation of type 1 collagen gels with purified recombinant murine FAP ECD alone (Fig. 9*B*, *lane 2*) failed to yield soluble collagen fragments. Collagen processing by FAP did require prior cleavage of collagen by MMP. Although unable to release fragments from intact collagen gels, FAP readily degraded MMP-generated ¾ and ¼ length collagen fragments to smaller fragments in a dose-dependent manner (Fig. 9*B*, *lanes 4–7*). The specificity of this finding was confirmed as pre-incubation with PT630, a FAP and DPPIV inhibitor (24), prevented subsequent digestion of the MMP-generated ¾ and ¼ length collagen fragments by FAP (Fig. 9*B*, *lane 8*).

These data indicate a direct role for FAP, in an ordered sequence with collagenase MMPs such as MMP1, in collagenolysis. Similar results were obtained with type III collagen (data not shown). MMP and MMP-FAP collagen digests were also resolved by HPLC and the fractions analyzed by gel electrophoresis (data not shown). This analysis demonstrated some degree of preservation of the quaternary structure of collagen, particularly in the MMP-only digests while also, to a lesser extent, following sequential digestion with MMP and FAP-ECD. HPLC also confirmed generation of an array of small collagen fragments from cleavage of ¾ and ¼ length fragments by FAP-ECD.

Intermediate-sized Collagen Fragments, Detectable in the Lungs of Wild-type Mice after Bleomycin, Are Present in the Lungs of FAP-deficient Mice at Baseline, Indicating a Defect in Collagen Turnover and Clearance—We sought evidence for FAP-dependent ordered proteolysis of collagen fragments *in vivo*. We postulated that intermediate-sized collagen fragments (*i.e.* ¾ and ¼ length fragments, for example) may persist longer in the extracellular matrix of FAP-null mice due to impaired collagen processing and turnover. To test this hypothesis, total lung ECM was isolated from mice 10 days after treatment with either saline or bleomycin via an established SDS-based decellularization protocol (37). Resolved lung ECM proteins were probed with a type I collagen antibody that recognizes various-sized collagen fragments as well as intact collagen. This analysis revealed increased intermediate-sized collagen fragments

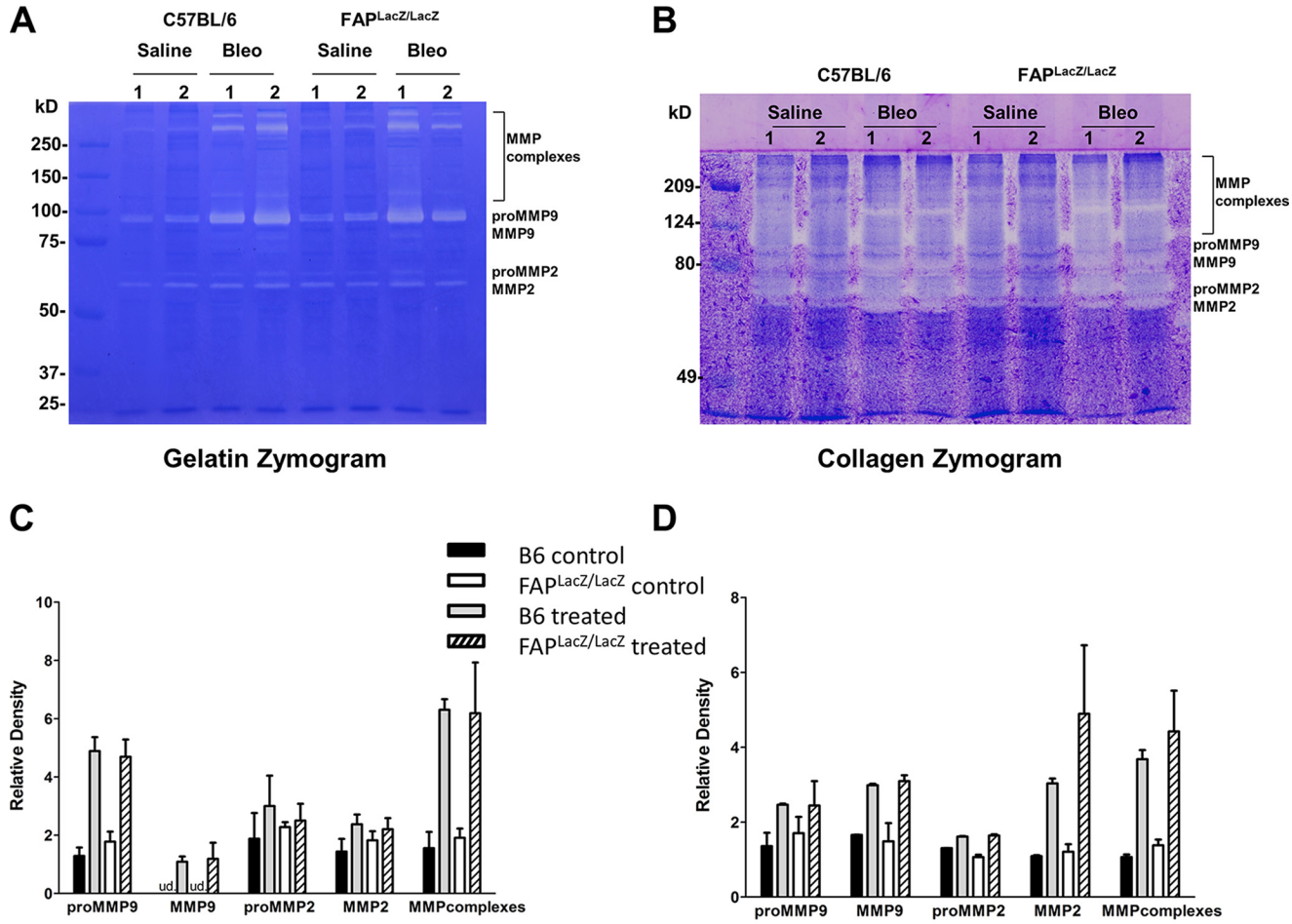

FIGURE 6. **MMPs are similarly induced in FAP$^{LacZ/LacZ}$ *versus* wild-type mice by intratracheal bleomycin.** *A,* representative gelatin zymogram showing MMP gelatinase activity in whole lung homogenates from FAP$^{LacZ/LacZ}$ *versus* wild-type mice 10 days after i.t. bleomycin (*Bleo*) (1.75 IU/kg) *versus* saline. $n = 5$ mice per group. 20 μg of protein was loaded per lane. *B,* representative collagen zymogram showing MMP collagenase activity in whole lung homogenates from FAP$^{LacZ/LacZ}$ *versus* wild-type mice 10 days after i.t. bleomycin *versus* saline. $n = 3$ mice per group. 50 μg of protein was loaded per lane. *C* and *D* show ImageJ densitometry quantification of bands seen in *A* and *B*, respectively.

(~70–120 and ~30–45 kDa) in the ECM isolated from FAP-null mice at baseline (Fig. 10*A*, *lane 2*). In contrast to lung ECM extracts from FAP-null mice, lung ECM extracts from untreated wild-type mice, which had similar levels of intact collagen, did not contain detectable levels of intermediate-sized collagen fragments at baseline (Fig. 10*A*, *1st lane*). After bleomycin, however, intermediate-sized collagen fragments were detectable in the wild-type lung ECM extracts (Fig. 10*A*, *3rd lane*). Interestingly, further increase in intermediate-sized collagen fragments was not evident in the FAP-null mice after bleomycin treatment (Fig. 10*A*, *4th lane*). Immunoblots for type I collagen in whole lung homogenates (Fig. 10*B*) from mice in our bleomycin experiments provided data very similar to our decellularized lung ECM extracts in Fig. 10*A*. Although intact collagen would not be present in these homogenates due to solubility issues, smaller, partially degraded collagen fragments should be soluble in standard lysis buffers and therefore recoverable. These blots do show an increase in type 1 collagen fragments (see ~60-kDa fragment) in the FAP-null mice at baseline, with a further increase in the ~60-kDa fragment with bleomycin treatment in both groups (Fig. 10*B*). These results echo what we saw in the ECM preparations made from decellularized lungs solubilized in protein extraction reagent 4 from Sigma (Fig 10*A*). We again, however, saw no significant difference in type I collagen fragment burden between the two bleomycin-treated groups. Bleomycin, in addition to causing a fibrotic response, also induces a strong inflammatory reaction. We suspect that in the bleomycin-treated animals, the influx of inflammatory cells, including phagocytes such as macrophages, may partially curb the accumulation of collagen fragments to some extent and make it difficult to appreciate subtle differences in the quantities of less abundant intermediate-sized collagen fragments.

FAP$^+$ Fibroblasts Demonstrate More Efficient Collagen Internalization than FAP-null Fibroblasts—Cleavage of intact collagen to smaller fragments facilitates its uptake into macrophages and fibroblasts and thereby accelerates matrix turnover. We postulated that collagen cleavage by cells expressing FAP on their surface contributes to efficient collagen internalization. Type I collagen was labeled with DyLight 650 to eliminate any issues with background autofluorescence from the primary lung fibroblasts or from collagen itself. We established that after labeling, the collagen was still amenable to cleavage by proteases (Fig 11*A*). FAP$^+$ wild-type primary mouse lung fibroblasts and FAP-null FAP$^{LacZ/LacZ}$ primary mouse lung fibroblasts were seeded on DL650 collagen gels in the presence of

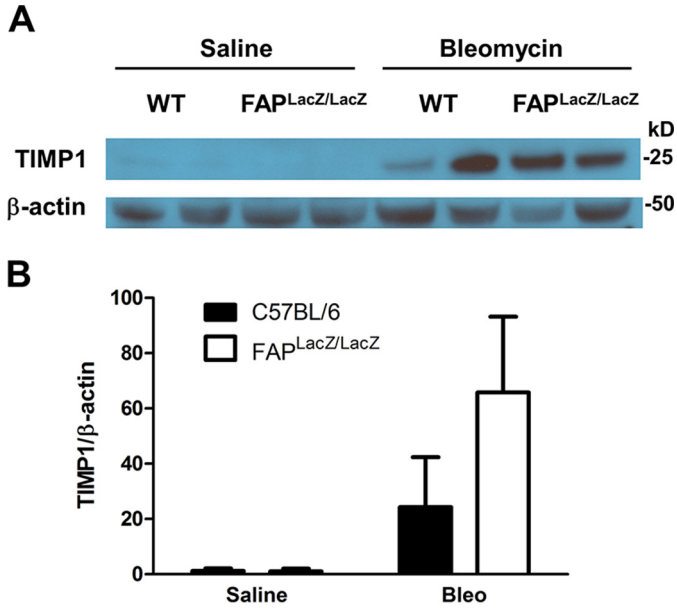

FIGURE 7. **TIMP1 is similarly induced at the protein level in FAP$^{LacZ/LacZ}$ *versus* wild-type mice after intratracheal bleomycin.** *A,* representative Western blot of whole lung homogenates from mice 10 days after intratracheal bleomycin (*Bleo*) (1.75 IU/kg) *versus* saline. *B,* ImageJ densitometry quantification of TIMP1 band intensity in saline *versus* bleomycin-treated mouse lung homogenates on Western blot, normalized to β-actin. $n = 3$ mice per saline-treated group; $n = 5$ mice per bleomycin-treated group.

lysosomal inhibitor E-64d and later recovered from the gels by collagenase/trypsin digest and seeded on fibronectin-coated glass coverslips for confocal microscopy examination. FAP$^+$ wild-type fibroblasts demonstrated greater uptake of DL650-labeled collagen by quantitative analysis (Fig. 11*B*). Treatment with a selective pharmacologic FAP inhibitor, *N*-(quinoline-4-carbonyl)-Gly-Pro(*F,F*)-nitrile, significantly decreased DL650-labeled collagen uptake by FAP$^+$ wild-type primary mouse lung fibroblasts (Fig. 11*D*). We evaluated for differences in expression of Endo180 (also known as uPARAP), the major receptor through which both intact and proteolytically cleaved fibrillary collagen is internalized and cleared by fibroblasts (44–47). Levels of Endo180 were similar between FAP$^+$ wild-type and FAP-null FAP$^{LacZ/LacZ}$ primary lung fibroblasts (Fig 11*C*). Processing and cleavage of intermediate-sized (*i.e.* ¾ and ¼) collagen fragments to smaller fragments by FAP thus directly facilitates collagen internalization by macrophages and fibroblasts, promoting matrix remodeling and restoration of lung homeostasis.

Reconstitution of FAP Expression by Adenoviral Gene Delivery Rescues FAP-deficient Mice and Decreases the Degree of Lung Fibrosis after Bleomycin Back to Levels of Wild-type Controls—Up to this point, we had shown that FAP deficiency predisposes to more severe lung fibrosis after injury in our bleomycin and thoracic irradiation models. To more directly show that FAP expression is protective in the murine lung, we performed reconstitution experiments. First, primary mouse lung fibroblasts derived from FAP$^{LacZ/LacZ}$ mice and wild-type controls (data not shown) were transduced with replication-deficient adenovirus expressing recombinant human FAP (adeno-hFAP) and empty vector (adeno-Y5). We confirmed robust hFAP expression 72 h later at a multiplicity of infection of 10 with further augmentation at a multiplicity of infection of 20 (Fig. 12*A*). No significant cellular toxicity was noted. We then established the effective dose of adeno-hFAP *in vivo*. 10^8 pfu of adeno-hFAP given via intratracheal injection was sufficient to cause robust hFAP expression at the mRNA (Fig. 12*B*) and protein (Fig. 12*C*) level by day 3 after adenovirus administration, which was relatively sustained, although there was some evidence that protein levels began to drop off by day 10 and definitely by day 15 (Fig. 12*C*, better appreciated in the FAP$^{LacZ/LacZ}$ IPIB, *upper blot*). This dose of adenovirus was well tolerated by the mice. A reconstitution experiment was then performed. FAP$^{LacZ/LacZ}$ mice and age/sex-matched wild-type controls were given 10^8 pfu adeno-hFAP *versus* adeno-Y5 via intratracheal injection followed by intratracheal bleomycin administration 72 h later. There was a significant reduction, back to levels similar to wild-type, in lung hydroxyproline content in the bleomycin-treated FAP$^{LacZ/LacZ}$ mice receiving i.t. adeno-hFAP compared with bleomycin-treated FAP$^{LacZ/LacZ}$ mice receiving adeno-Y5 (Fig. 12*D*), amounting to rescue of the FAP-deficient phenotype with FAP overexpression. Bleomycin-treated wild-type mice receiving adeno-hFAP had equivalent lung hydroxyproline content to bleomycin-treated wild-type mice receiving adeno-Y5, so FAP overexpression beyond a certain point did not seem to confer additional benefit. Some limitations of the adenoviral overexpression approach may have affected our findings, namely the induction of ectopic FAP expression in lung epithelial cells as well as possibly other cell types besides lung fibroblasts, and also the unavoidable acute bystander inflammation induced by the adenoviral infection itself.

Discussion

In our ever-aging population, morbidity and mortality from pulmonary fibrosis continues to rise, with overall mortality from pulmonary fibrosis now outstripping that associated with several malignancies such as bladder cancer, acute myelogenous leukemia, and multiple myeloma (48). Without question, there is a compelling need for better insight into the events that govern the conversion of what begins as a normal healing process after lung injury into an uncontrolled fibroproliferative response resulting in irreversible scarring, tissue distortion, and progressive decline in lung function.

The scientific literature supports a role for aberrant regulation of cell surface and matrix-associated proteases in the pathogenesis of pulmonary fibrosis (49–52). MMPs (49, 50, 53), neutrophil elastase (54, 55), and proteinases of the coagulation cascade (56–60) have all been implicated in the disease. Although the balance of the literature to date indicates a profibrotic action of these particular proteases, we have found that FAP, a serine protease in the DPP family, exerts a protective anti-fibrotic effect in the setting of lung injury. This may at first seem counterintuitive as proteins up-regulated in disease tend to serve a pathologic role. However, the scientific literature catalogues a growing number of proteins up-regulated in disease that work to counter the disease process, reestablish homeostasis, and return the body to its original state of health (61–63), and we have found that FAP behaves in such a fashion in pulmonary fibrosis.

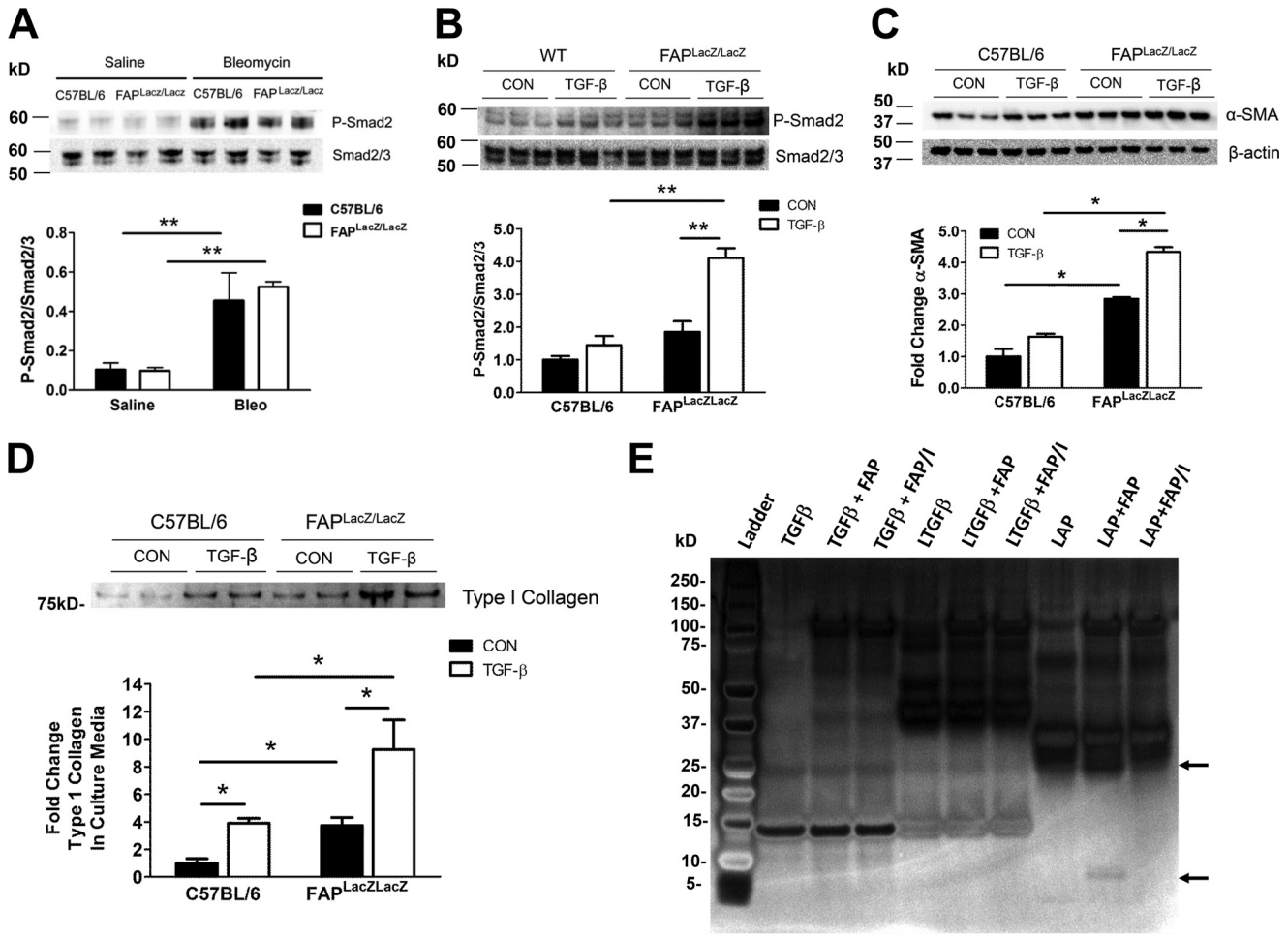

FIGURE 8. **Although overall activation of the TGF-β pathway appears similar in the lungs of FAP$^{LacZ/LacZ}$ *versus* wild-type mice after i.t. bleomycin administration, FAP-deficient fibroblasts develop a more robust myofibroblast phenotype in response to TGF-β compared with wild-type.** *A,* representative immunoblot of phospho-Smad2 normalized to total Smad 2/3 in whole lung homogenates from mice 14 days after i.t. bleomycin (*Bleo*) (1.75 IU/kg) *versus* saline. Densitometry was performed by ImageJ. $n = 3$ mice per group. ** indicates $p < 0.01$. *B* and *C,* primary mouse lung fibroblasts derived from FAP$^{Lac/LacZ}$ *versus* wild-type mice were cultured on collagen-coated plates and treated with TGF-β (10 ng/ml) *versus* vehicle control. *B,* representative immunoblot for phospho-Smad2 *versus* total Smad2/3 after 90 min TGF-β *versus* vehicle control (*CON*) exposure. *C,* representative immunoblot for α-SMA normalized to β-actin after 48 h of TGF-β stimulation *versus* vehicle control. *D,* primary mouse lung fibroblasts derived from FAP$^{Lac/LacZ}$ *versus* wild-type mice were cultured on uncoated plates and treated with TGF-β (10 ng/ml) *versus* vehicle control. Cell culture media were assessed 72 h later for the presence of type 1 collagen fragments. A representative immunoblot is shown. *B–D,* densitometry for these fibroblast experiments was performed by ImageJ. $n = 3$ independent samples per group. * indicates $p < 0.05$; ** indicates $p < 0.01$. All fibroblast experiments were repeated in triplicate. *E,* FAP does not cleave active or latent TGF-β but does cleave LAP to some extent. 1 μg of 1) active recombinant human TGF-β (TGFβ), 2) latent TGF-β (LTGFβ), and 3) recombinant human LAP were incubated at 37 °C for 16 h either 1) alone, 2) with 2.5 μg of recombinant murine FAP (FAP), or 3) with 2.5 μg of recombinant murine FAP preincubated with a selective FAP inhibitor, *N*-(quinolone-4-carbonyl)-Gly-Pro(*F,F*)-nitrile (FAP/I), for 15 min. Samples were then resolved on a 4–12% Bis-Tris gel and stained with colloidal silver. *Black arrows* highlight new bands indicating a small degree of cleavage of LAP by FAP.

This study is the first to demonstrate that the absence of FAP worsens the development of pulmonary fibrosis after lung injury, establishing a protective role for FAP in the lung. In designing the murine studies that ultimately led to this conclusion, we elected to conduct both thoracic irradiation and i.t. bleomycin experiments because the two fibrosis models complement each other. Bleomycin gives us insight into events earlier in the development of pulmonary fibrosis, when dysregulated lung remodeling and matrix deposition may be reversible, whereas thoracic irradiation allows us to study chronic and more advanced stages of disease. We did not necessarily expect the two models to yield the same outcomes. In the end, however, FAP-deficient mice experienced decreased survival and increased fibrosis compared with wild type in both models, which validates and strengthens our findings.

Very simplistically, fibrosis can be understood as an imbalance between collagen synthesis and collagen catabolism and clearance. Although much ongoing effort has been appropriately directed at studying the activated fibroblast/myofibroblast as the prime mediator(s) of collagen overproduction in fibrosis, less examination has been given to the competing events of matrix remodeling, collagen turnover, and scar resorption. Collagen turnover has been described to occur through two processes, somewhat interrelated. The first is the extracellular/pericellular proteolytic cleavage of collagen, classically by MMPs with collagenase (*i.e.* MMP1, -8, -13, and -14) followed by those with gelatinase (*i.e.* MMP2 and -9) activity, although other proteases likely participate as well, including FAP as indicated by our current study (64–67). The second event involves endocytosis of collagen

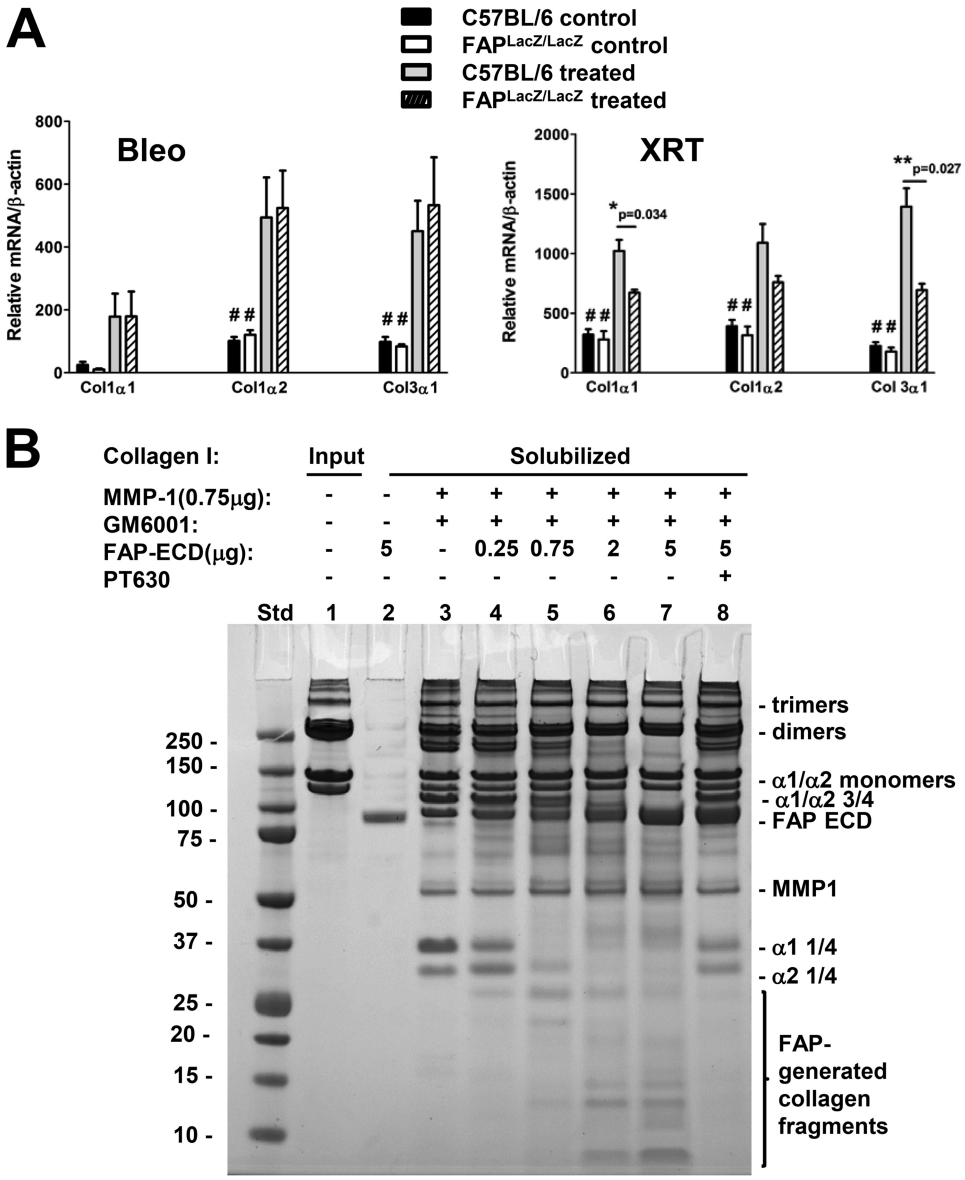

FIGURE 9. **FAP mediates degradation of MMP1-derived collagen cleavage products *in vitro*.** *A,* relative lung Col1α1, Col1α2, and Col3α1 mRNA levels in FAP$^{LacZ/LacZ}$ and wild-type mice 7 days after i.t. bleomycin (*Bleo*) (treated) *versus* saline (control) or 16 weeks after 13.5 Gy thoracic irradiation (treated) *versus* no treatment (control), normalized to β-actin. #, $p < 0.05$ comparing control *versus* treated groups for the designated genotype. *, $p < 0.05$ comparing genotypes within the designated treatment group. *B,* type I collagen digests with recombinant MMP1 ± recombinant murine FAP extracellular domain (rFAP-ECD). Rat tail type I collagen was untreated (input, *lane 1*) or solidified and then digested with rFAP-ECD alone (*lane 2*) or with 0.75 μg of recombinant human MMP-1 (*lanes 3–8*). In *lanes 3–8*, GM6001 was added after 8 h to halt further MMP activity, and then further digestion was performed with the indicated microgram amounts of purified rFAP-ECD (*lanes 4–8*) for an additional 8 h in the absence (*lanes 4–7*) or presence of the FAP inhibitor PT630 (*lane 8*). The soluble fraction was then resolved on a 4–12% Bis-Tris gel and stained with Coomassie Blue.

through interaction with cell surface receptors, in particular $\alpha_2\beta_1$ integrin and uPARAP/Endo180, with subsequent degradation of the internalized collagen within the lysosomal compartment (45, 47, 68–70). Although intact collagen may be endocytosed, fragmentation of collagen greatly speeds its rate of internalization and clearance (44, 71). Collagen internalization through uPARAP/Endo180 has been implicated in both tumorigenesis and the development of fibrosis in the liver and lung *in vivo* (46, 47, 72).

Our study establishes an important role for FAP in collagen clearance and matrix turnover. Although FAP is unable to cleave intact type 1 collagen, our *in vitro* assay clearly demonstrates the ability of FAP to process ¾ and ¼ length collagen fragments generated by prior MMP exposure into smaller degradation products, facilitating their clearance. We were able to detect intermediate-sized collagen fragments in total lung ECM preparations as well as in whole lung homogenates from FAP-null mice at baseline, although these mid-sized collagen fragments were absent in lung ECM extracts and less abundant in whole lung homogenates from saline-treated wild-type mice. These data suggest that animals lacking FAP activity have a defect in collagen catabolism even under homeostatic conditions, hence collagen fragments that are normally not present in detectable quantities or at least present at very low levels are found accumulating in the FAP-null mice. Both wild-type and FAP-null mice demonstrated the presence of

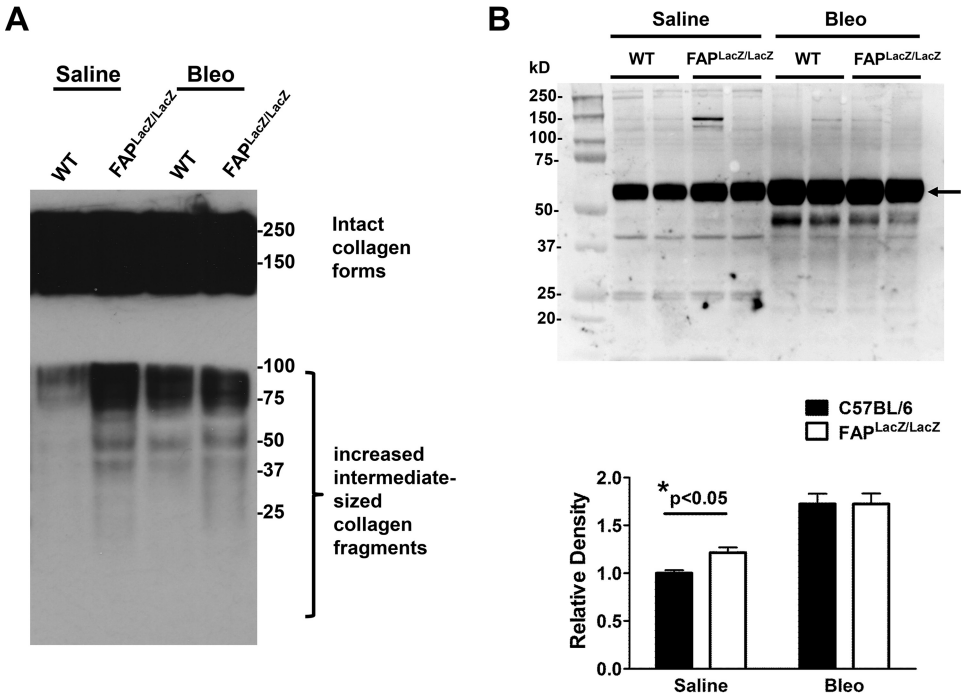

FIGURE 10. **FAP deficiency leads to accumulation of partially processed intermediate-sized collagen fragments *in vivo*.** *A,* representative immunoblot for type 1 collagen in decellularized lung ECM extracts from wild-type and $FAP^{LacZ/LacZ}$ mice 10 days after i.t. bleomycin *versus* saline. Equal amounts of protein were resolved on 3–8% Tris acetate (not shown here) and 4–12% Bis-Tris gels and then probed for type 1 collagen. Lung ECM sample order is as follows: *1st lane*, WT saline-treated; *2nd lane*, FAP-null saline-treated; *3rd lane*, WT bleo-treated; *4th lane*, FAP-null bleomycin (*Bleo*)-treated. This experiment was repeated in triplicate. *B,* representative immunoblot of whole lung homogenates from mice 14 days after i.t. bleomycin (1.0 IU/kg) *versus* saline resolved on a 4–12% Bis-Tris gel and probed for type 1 collagen. *Black arrow* indicates ~60-kDa fragment quantified by densitometry (ImageJ) below. $n = 3$ independent samples per group. * indicates $p < 0.05$.

intermediate-sized collagen fragments in lung ECM extracts and whole lung homogenates after i.t. bleomycin, likely related to increased collagen turnover in the setting of lung injury. In wild-type mice, we reason that these fragments appear after bleomycin treatment because the accelerated rate of collagen turnover in the setting of inflammation, scarring, and increased collagen production and fibrosis exceeds the enzymatic limits of FAP and other gelatinases present in tissues. This allows these intermediate-sized collagen fragments to be transiently seen, whereas under normal circumstances they would not be detectable.

Many might question whether FAP plays a significant role in collagen degradation *in vivo*, because multiple MMPs possessing gelatinase activity similarly cleave ¾ and ¼ length collagen fragments into smaller fragments indicating some redundancy of function. However, the detection of intermediate-sized collagen fragments in lung ECM isolated from FAP-null mice but not from B6 wild-type mice indicates that FAP indeed plays a significant role in collagen turnover *in vivo*, because its absence alters collagen composition. A recent study from our laboratory also supports a role for FAP in collagen turnover as CD26 tumors in FAP-null mice demonstrate dramatically increased amounts of collagen stroma as do tumors in wild-type mice in which the enzymatic activity of FAP has been pharmacologically inhibited (24). Furthermore, our finding that FAP^+ fibroblasts more effectively internalize collagen compared with FAP-null cells confirms an important functional role for the protein in fibrogenesis. Our data are supported by a recent independent study where a genome-wide RNA interference screen in *Drosophila* S2 cells identified FAP as one of 22 candidate genes associated with increased collagen uptake (73). Finally, our data showing that FAP expression appears to modulate TGF-β-mediated myofibroblast differentiation suggests that FAP may be very important in regulating the fibrogenic response after lung injury. On the basis of these results, we propose that FAP plays a larger role in ECM remodeling *in vivo* than has been previously appreciated, commensurate and in concert with the more widely studied MMPs.

Our study has several important implications. It points to a previously unrecognized, essential role for FAP in matrix remodeling and collagen clearance in the lung and identifies FAP as a novel endogenous regulator of fibrosis. Although a better understanding of myofibroblast biology might allow one to turn off collagen production by this cell type, the ability to accelerate collagen degradation could mean not only halting further scar formation but achieving resorption of collagen and reversal of established fibrosis. This has major implications for the field of pulmonary medicine, in particular interstitial lung disease. Having shown FAP to play a protective, homeostatic role in the lung, promoting resorption of scar by direct participation in collagen catabolism and clearance and dampening myofibroblast induction in response to TGF-β, we now may consider ways to increase FAP expression, enhance enzymatic activity, and/or target downstream effectors in the future to try to minimize the development of lung fibrosis in certain scenarios.

Our study has important ramifications for cancer biology. FAP is already a protein of great interest in the cancer field, with

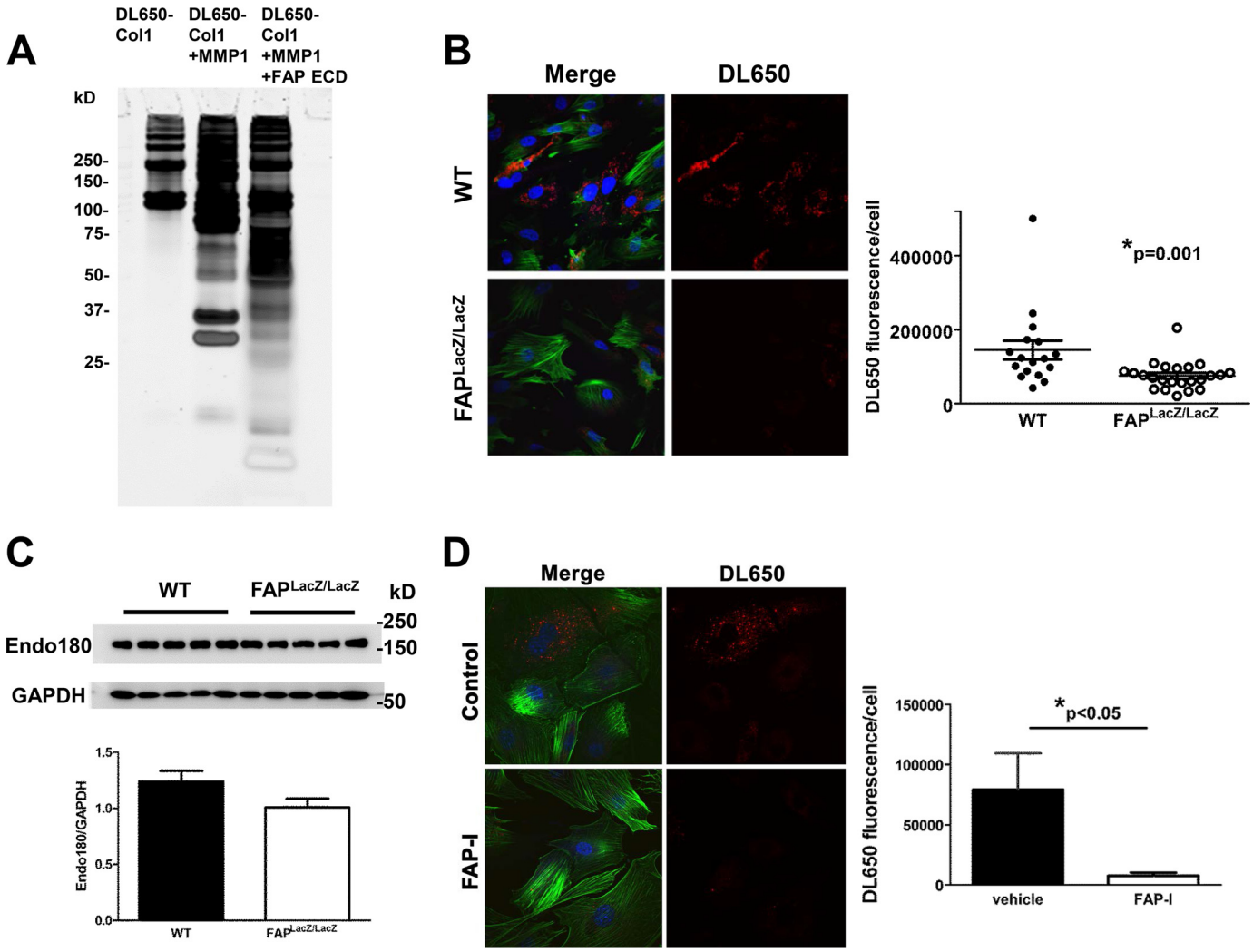

FIGURE 11. **FAP$^+$ wild-type primary lung fibroblasts internalize type I collagen more efficiently than FAP-null fibroblasts.** *A,* DL650-labeled collagen (intact, unpolymerized, *1st lane*) *versus* MMP-1-digested (*2nd lane*) *versus* MMP-1 followed by FAP ECD-digested (*3rd lane*) DL650-labeled collagen were resolved on a 4–12% Bis-Tris gel, and the gel was imaged in the Cy5 channel by a Typhoon imager. Fluorescent labeling did not impede proteolytic degradation of the collagen. *B,* primary mouse lung fibroblasts derived from FAP$^+$ wild-type and FAP-null FAP$^{LacZ/LacZ}$ mice were seeded on DL650-labeled collagen gels for 9 h, in the presence of E-64d, a lysosomal inhibitor, then recovered by collagenase/trypsin digest, seeded on fibronectin-coated glass coverslips, and examined by confocal microscopy. DL650 fluorescence/cell was quantified by Metamorph software. *Red,* internalized DL650-labeled collagen; *blue,* Hoechst dye; *green,* F-actin. *C,* cell lysates from untreated primary mouse lung fibroblasts (P3) derived from FAP$^+$ wild-type and FAP-null FAP$^{LacZ/LacZ}$ mice were probed for the collagen receptor, Endo180; reference protein GAPDH. $n = 5$ independent samples per group. *D,* pretreatment of primary wild-type mouse lung fibroblasts with a selective FAP inhibitor, *N*-(quinoline-4-carbonyl)-Gly-Pro(*F,F*)-nitrile, significantly reduces collagen internalization by FAP$^+$ fibroblasts. Primary mouse lung fibroblasts derived from FAP$^+$ wild-type mice were pretreated for an hour and then maintained in the selective FAP inhibitor, *N*-(quinoline-4-carbonyl)-Gly-Pro(*F,F*)-nitrile, or vehicle control at 1 mM concentration for the duration of the experiment. After pretreatment, primary mouse lung fibroblasts were seeded on DL650-labeled collagen gels for 9 h, in the presence of E-64d, a lysosomal inhibitor, then recovered by collagenase/trypsin digest, seeded on fibronectin-coated glass coverslips, and examined by confocal microscopy. DL650 fluorescence/cell was quantified by NIS Elements software. *Red,* internalized DL650-labeled collagen; *blue,* Hoechst dye; *green,* F-actin.

many groups working on potential means of safe pharmacologic inhibition of FAP to target the tumor microenvironment or stroma. In light of our findings, however, one must proceed with somewhat heightened caution in such endeavors. Many patients with primary lung cancers or other intrathoracic malignancies undergo adjuvant radiation therapy for local tumor control and/or chemotherapy. If future treatment regimens include a pharmacologic inhibitor of FAP, we need to ensure that patients will not be at increased risk of developing radiation-induced or chemotherapy-related interstitial lung disease. A better understanding of the role of FAP in human fibrosing conditions is required.

The potential biological significance of the intermediate-sized collagen fragments that accumulate in FAP-null animals at baseline and in both genotypes after lung injury should also be mentioned. Previous work by others has shown significant biological activity of peptides generated from proteolytic degradation of collagens, for example the chemotactic properties of the matrikine, PGP, or the antifibrotic actions of endostatin, a product of proteolytic degradation of collagen XVIII (61, 74, 75). Indeed, we did identify increased neutrophilic inflammation in BAL fluid from FAP-null mice compared with wild type in our bleomycin model as well as a more prominent inflammatory infiltrate overall in the BAL from FAP-null mice *versus* wild type after thoracic

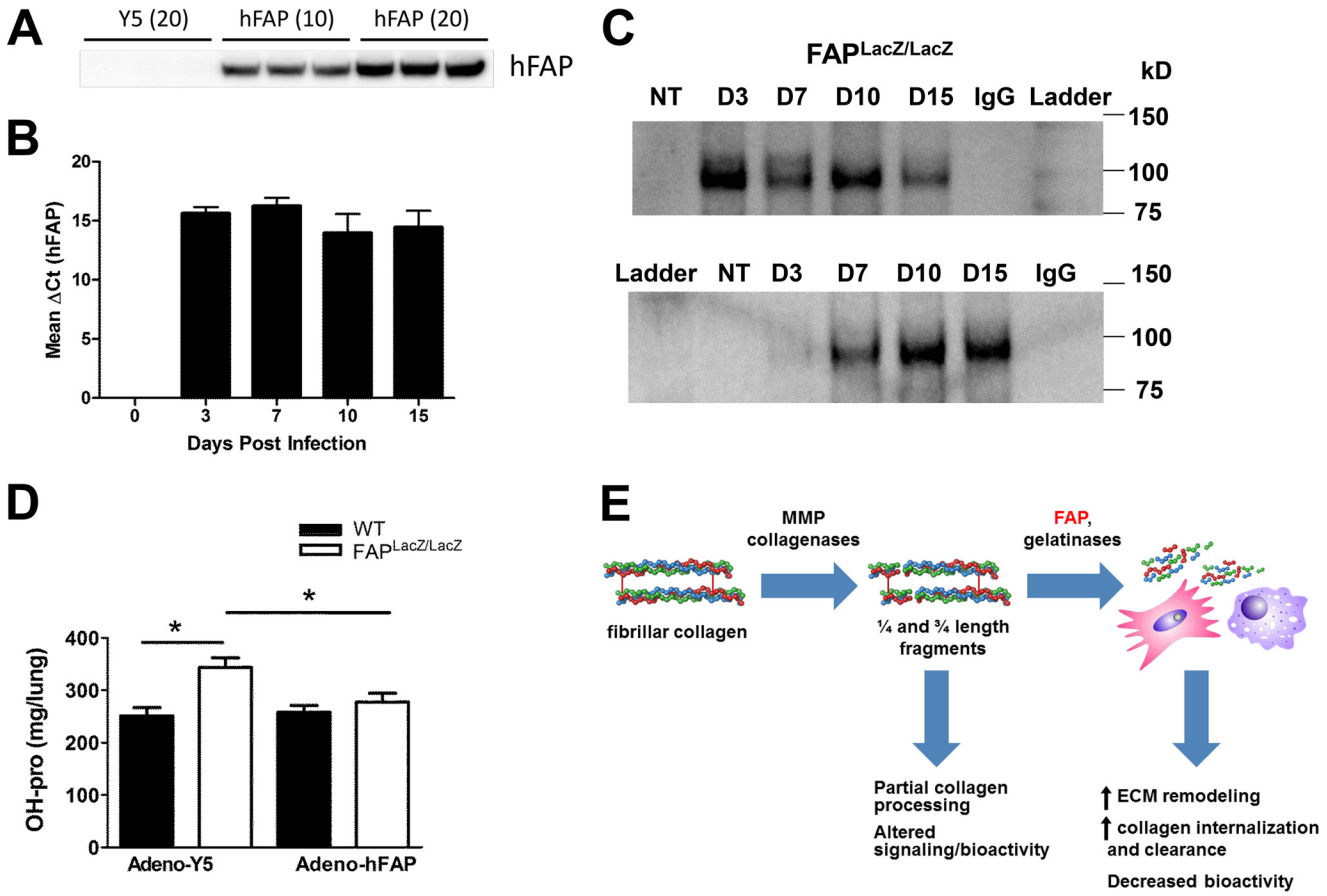

FIGURE 12. **Adenovirus-mediated reconstitution of lung FAP expression significantly reduces lung collagen content and fibrosis in FAP-deficient mice after i.t. bleomycin.** *A*, FAP-deficient $FAP^{LacZ/LacZ}$ mouse lung fibroblasts were transduced with adenovirus expressing recombinant human FAP (adeno-hFAP) *versus* empty vector (adeno-Y5). Cells were harvested 72 h later and immunoblotted for hFAP. $n = 3$/group. The multiplicity of infection is indicated in *parentheses*. *B–D*, $FAP^{LacZ/LacZ}$ mice and age/sex-matched C57BL/6 controls received 10^8 pfu of adeno-hFAP *versus* adeno-Y5 via intratracheal injection. *B*, lung hFAP mRNA expression over time in mice who received i.t. adeno-hFAP. $n = 3$ mice/group. *C*, IPIB showing lung hFAP expression in $FAP^{LacZ/LacZ}$ (*top blot*) and C57BL/6 wild-type mice (*bottom blot*) over time after i.t. adeno-hFAP administration. *D*, 72 h after i.t. adenovirus (10^8 pfu) administration, mice were treated with i.t. bleomycin 1.0 IU/kg. Hydroxyproline content/R lung was assessed 15 days after bleomycin treatment. $n = 6–10$ mice per group. * indicates $p < 0.05$. *E*, schematic of our working hypothesis for FAP's role in ECM remodeling and fibrosis.

irradiation (data not shown). So beyond the simple physical accumulation of collagen and collagen fragments within the interstitium of the lung in the absence of FAP, one must also consider the possibility that the presence or absence of certain products of ECM turnover and their biological effects may contribute to enhanced fibrogenesis as well (see proposed schema, Fig. 12*E*). Finally, it is possible, and perhaps even likely, that FAP may cleave other essential proteins involved in the pathogenesis of pulmonary fibrosis besides collagens and influence the development of the disease through yet another mechanism.

Author Contributions—M. H. F., M. C. S., and E. P. designed the experiments. M. H. F., Q. Z., and H. H. L. performed the majority of the experiments, with later additional technical assistance from D. L. G. and J. A. J. H. J. R. assisted with the zymography in Fig. 6, and S. M. performed the α-SMA immunofluorescence staining in Fig. 4. D. H. M., M. C. S., D. W. S., C. F. B., and W. W. B. each contributed scientific expertise that refined our experimental methods and approach. W. W. B. also generously provided us with the selective FAP inhibitor, *N*-(quinoline-4-carbonyl)-Gly-Pro(*F,F*)-nitrile, for our fibroblast studies. M. H. F. wrote the manuscript, and all co-authors contributed to its revision and attest to the accuracy and integrity of the work.

Acknowledgments—We acknowledge and thank Boehringer-Ingelheim for sharing the original FAP-null $FAP^{LacZ/LacZ}$ mouse with us, Dr. Jonathan Cheng for supplying HEK293 cells transfected with murine FAP ECD-containing plasmid, and the Ludwig Institute for Cancer Research for sharing the F19 anti-hFAP antibody. We thank Dr. Sergey Leikin for sharing his vast expertise on collagen biology, techniques for isolating, labeling, and working with collagen, and for the careful review of the manuscript. We also thank Dr. Jinghua Zhu and Dr. Merry L. Lindsey (University of Texas, San Antonio) for sharing their protocol for ECM isolation and their helpful technical advice. We thank Evguenia Arguiri from Dr. Melpo Christofidou-Solomidou's laboratory for assistance with the thoracic irradiation experiments. We thank Frederick Keeney and James Hayden (The Wistar Institute Microscopy Core) and Simon Watkins, Callen Wallace, and Claudette St. Croix (Center for Biologic Imaging (University of Pittsburgh)) for their invaluable assistance. We also thank Terri Dobranksy for her computer graphics assistance in the creation of our schematic in Fig. 12E.

References

1. Ley, B., Collard, H. R., and King, T. E., Jr. (2011) Clinical course and prediction of survival in idiopathic pulmonary fibrosis. *Am. J. Respir. Crit. Care. Med.* **183,** 431–440

2. Richeldi, L., du Bois, R. M., Raghu, G., Azuma, A., Brown, K. K., Costabel, U., Cottin, V., Flaherty, K. R., Hansell, D. M., Inoue, Y., Kim, D. S., Kolb, M., Nicholson, A. G., Noble, P. W., Selman, M., *et al.* (2014) Efficacy and safety of nintedanib in idiopathic pulmonary fibrosis. *N. Engl. J. Med.* **370,** 2071–2082
3. King, T. E., Jr., Bradford, W. Z., Castro-Bernardini, S., Fagan, E. A., Glaspole, I., Glassberg, M. K., Gorina, E., Hopkins, P. M., Kardatzke, D., Lancaster, L., Lederer, D. J., Nathan, S. D., Pereira, C. A., Sahn, S. A., Sussman, R., *et al.* (2014) A phase 3 trial of pirfenidone in patients with idiopathic pulmonary fibrosis. *N. Engl. J. Med.* **370,** 2083–2092
4. Karimi-Shah, B. A., and Chowdhury, B. A. (2015) Forced vital capacity in idiopathic pulmonary fibrosis–FDA review of pirfenidone and nintedanib. *N. Engl. J. Med.* **372,** 1189–1191
5. Scanlan, M. J., Raj, B. K., Calvo, B., Garin-Chesa, P., Sanz-Moncasi, M. P., Healey, J. H., Old, L. J., and Rettig, W. J. (1994) Molecular cloning of fibroblast activation protein α, a member of the serine protease family selectively expressed in stromal fibroblasts of epithelial cancers. *Proc. Natl. Acad. Sci. U.S.A.* **91,** 5657–5661
6. Acharya, P. S., Zukas, A., Chandan, V., Katzenstein, A. L., and Puré, E. (2006) Fibroblast activation protein: a serine protease expressed at the remodeling interface in idiopathic pulmonary fibrosis. *Hum. Pathol.* **37,** 352–360
7. Meadows, S. A., Edosada, C. Y., Mayeda, M., Tran, T., Quan, C., Raab, H., Wiesmann, C., and Wolf, B. B. (2007) Ala657 and conserved active site residues promote fibroblast activation protein endopeptidase activity via distinct mechanisms of transition state stabilization. *Biochemistry* **46,** 4598–4605
8. Piñeiro-Sánchez, M. L., Goldstein, L. A., Dodt, J., Howard, L., Yeh, Y., Tran, H., Argraves, W. S., and Chen, W. T. (1997) Identification of the 170-kDa melanoma membrane-bound gelatinase (seprase) as a serine integral membrane protease. *J. Biol. Chem.* **272,** 7595–7601
9. Aggarwal, S., Brennen, W. N., Kole, T. P., Schneider, E., Topaloglu, O., Yates, M., Cotter, R. J., and Denmeade, S. R. (2008) Fibroblast activation protein peptide substrates identified from human collagen I derived gelatin cleavage sites. *Biochemistry* **47,** 1076–1086
10. Niedermeyer, J., Garin-Chesa, P., Kriz, M., Hilberg, F., Mueller, E., Bamberger, U., Rettig, W. J., and Schnapp, A. (2001) Expression of the fibroblast activation protein during mouse embryo development. *Int. J. Dev. Biol.* **45,** 445–447
11. Mathew, S., Scanlan, M. J., Mohan Raj, B. K., Murty, V. V., Garin-Chesa, P., Old, L. J., Rettig, W. J., and Chaganti, R. S. (1995) The gene for fibroblast activation protein α (FAP), a putative cell surface-bound serine protease expressed in cancer stroma and wound healing, maps to chromosome band 2q23. *Genomics* **25,** 335–337
12. Wang, X. M., Yao, T. W., Nadvi, N. A., Osborne, B., McCaughan, G. W., and Gorrell, M. D. (2008) Fibroblast activation protein and chronic liver disease. *Front. Biosci.* **13,** 3168–3180
13. Levy, M. T., McCaughan, G. W., Abbott, C. A., Park, J. E., Cunningham, A. M., Müller, E., Rettig, W. J., and Gorrell, M. D. (1999) Fibroblast activation protein: a cell surface dipeptidyl peptidase and gelatinase expressed by stellate cells at the tissue remodelling interface in human cirrhosis. *Hepatology* **29,** 1768–1778
14. Park, J. E., Lenter, M. C., Zimmermann, R. N., Garin-Chesa, P., Old, L. J., and Rettig, W. J. (1999) Fibroblast activation protein, a dual specificity serine protease expressed in reactive human tumor stromal fibroblasts. *J. Biol. Chem.* **274,** 36505–36512
15. Huber, M. A., Kraut, N., Park, J. E., Schubert, R. D., Rettig, W. J., Peter, R. U., and Garin-Chesa, P. (2003) Fibroblast activation protein: differential expression and serine protease activity in reactive stromal fibroblasts of melanocytic skin tumors. *J. Invest. Dermatol.* **120,** 182–188
16. Cohen, S. J., Alpaugh, R. K., Palazzo, I., Meropol, N. J., Rogatko, A., Xu, Z., Hoffman, J. P., Weiner, L. M., and Cheng, J. D. (2008) Fibroblast activation protein and its relationship to clinical outcome in pancreatic adenocarcinoma. *Pancreas* **37,** 154–158
17. Monsky, W. L., Lin, C. Y., Aoyama, A., Kelly, T., Akiyama, S. K., Mueller, S. C., and Chen, W. T. (1994) A potential marker protease of invasiveness, seprase, is localized on invadopodia of human malignant melanoma cells. *Cancer Res.* **54,** 5702–5710
18. Chung, K. M., Hsu, S. C., Chu, Y. R., Lin, M. Y., Jiaang, W. T., Chen, R. H., and Chen, X. (2014) Fibroblast activation protein (FAP) is essential for the migration of bone marrow mesenchymal stem cells through RhoA activation. *PLoS One* **9,** e88772
19. Bae, S., Park, C. W., Son, H. K., Ju, H. K., Paik, D., Jeon, C. J., Koh, G. Y., Kim, J., and Kim, H. (2008) Fibroblast activation protein α identifies mesenchymal stromal cells from human bone marrow. *Br. J. Haematol.* **142,** 827–830
20. Arnold, J. N., Magiera, L., Kraman, M., and Fearon, D. T. (2014) Tumoral immune suppression by macrophages expressing fibroblast activation protein-α and heme oxygenase-1. *Cancer Immunol. Res.* **2,** 121–126
21. Tchou, J., Zhang, P. J., Bi, Y., Satija, C., Marjumdar, R., Stephen, T. L., Lo, A., Chen, H., Mies, C., June, C. H., Conejo-Garcia, J., and Puré, E. (2013) Fibroblast activation protein expression by stromal cells and tumor-associated macrophages in human breast cancer. *Hum. Pathol.* **44,** 2549–2557
22. Christiansen, V. J., Jackson, K. W., Lee, K. N., and McKee, P. A. (2007) Effect of fibroblast activation protein and α2-antiplasmin cleaving enzyme on collagen types I, III, and IV. *Arch. Biochem. Biophys.* **457,** 177–186
23. Brokopp, C. E., Schoenauer, R., Richards, P., Bauer, S., Lohmann, C., Emmert, M. Y., Weber, B., Winnik, S., Aikawa, E., Graves, K., Genoni, M., Vogt, P., Lüscher, T. F., Renner, C., Hoerstrup, S. P., and Matter, C. M. (2011) Fibroblast activation protein is induced by inflammation and degrades type I collagen in thin-cap fibroatheromata. *Eur. Heart J.* **32,** 2713–2722
24. Santos, A. M., Jung, J., Aziz, N., Kissil, J. L., and Puré, E. (2009) Targeting fibroblast activation protein inhibits tumor stromagenesis and growth in mice. *J. Clin. Invest.* **119,** 3613–3625
25. Iwasa, S., Okada, K., Chen, W. T., Jin, X., Yamane, T., Ooi, A., and Mitsumata, M. (2005) Increased expression of seprase, a membrane-type serine protease, is associated with lymph node metastasis in human colorectal cancer. *Cancer Lett.* **227,** 229–236
26. Cheng, J. D., Dunbrack, R. L., Jr., Valianou, M., Rogatko, A., Alpaugh, R. K., and Weiner, L. M. (2002) Promotion of tumor growth by murine fibroblast activation protein, a serine protease, in an animal model. *Cancer Res.* **62,** 4767–4772
27. Henry, L. R., Lee, H. O., Lee, J. S., Klein-Szanto, A., Watts, P., Ross, E. A., Chen, W. T., and Cheng, J. D. (2007) Clinical implications of fibroblast activation protein in patients with colon cancer. *Clin. Cancer Res.* **13,** 1736–1741
28. Niedermeyer, J., Kriz, M., Hilberg, F., Garin-Chesa, P., Bamberger, U., Lenter, M. C., Park, J., Viertel, B., Püschner, H., Mauz, M., Rettig, W. J., and Schnapp, A. (2000) Targeted disruption of mouse fibroblast activation protein. *Mol. Cell. Biol.* **20,** 1089–1094
29. Moore, B. B., and Hogaboam, C. M. (2008) Murine models of pulmonary fibrosis. *Am. J. Physiol. Lung Cell. Mol. Physiol.* **294,** L152–L160
30. National Research Council (United States) Committee for the Update of the Guide for the Care and Use of Laboratory Animals (2011) *Guide for the Care and Use of Laboratory Animals*, 8th Ed., pp. 1–220, National Academies Press, Washington, D.C.
31. Machtay, M., Scherpereel, A., Santiago, J., Lee, J., McDonough, J., Kinniry, P., Arguiri, E., Shuvaev, V. V., Sun, J., Cengel, K., Solomides, C. C., and Christofidou-Solomidou, M. (2006) Systemic polyethylene glycol-modified (PEGylated) superoxide dismutase and catalase mixture attenuates radiation pulmonary fibrosis in the C57/bl6 mouse. *Radiother. Oncol.* **81,** 196–205
32. Wang, L. C., Lo, A., Scholler, J., Sun, J., Majumdar, R. S., Kapoor, V., Antzis, M., Cotner, C. E., Johnson, L. A., Durham, A. C., Solomides, C. C., June, C. H., Puré, E., and Albelda, S. M. (2014) Targeting fibroblast activation protein in tumor stroma with chimeric antigen receptor T cells can inhibit tumor growth and augment host immunity without severe toxicity. *Cancer Immunol. Res.* **2,** 154–166
33. Sulek, J., Wagenaar-Miller, R. A., Shireman, J., Molinolo, A., Madsen, D. H., Engelholm, L. H., Behrendt, N., and Bugge, T. H. (2007) Increased expression of the collagen internalization receptor uPARAP/Endo180 in the stroma of head and neck cancer. *J. Histochem. Cytochem.* **55,** 347–353
34. Gogly, B., Groult, N., Hornebeck, W., Godeau, G., and Pellat, B. (1998) Collagen zymography as a sensitive and specific technique for the deter-

mination of subpicogram levels of interstitial collagenase. *Anal. Biochem.* **255,** 211–216
35. Ott, H. C., Matthiesen, T. S., Goh, S. K., Black, L. D., Kren, S. M., Netoff, T. I., and Taylor, D. A. (2008) Perfusion-decellularized matrix: using nature's platform to engineer a bioartificial heart. *Nat. Med.* **14,** 213–221
36. DeQuach, J. A., Mezzano, V., Miglani, A., Lange, S., Keller, G. M., Sheikh, F., and Christman, K. L. (2010) Simple and high yielding method for preparing tissue specific extracellular matrix coatings for cell culture. *PLoS One* **5,** e13039
37. de Castro Brás, L. E., Ramirez, T. A., DeLeon-Pennell, K. Y., Chiao, Y. A., Ma, Y., Dai, Q., Halade, G. V., Hakala, K., Weintraub, S. T., and Lindsey, M. L. (2013) Texas 3-step decellularization protocol: looking at the cardiac extracellular matrix. *J. Proteomics* **86,** 43–52
38. Acharya, P. S., Majumdar, S., Jacob, M., Hayden, J., Mrass, P., Weninger, W., Assoian, R. K., and Puré, E. (2008) Fibroblast migration is mediated by CD44-dependent TGF β activation. *J. Cell Sci.* **121,** 1393–1402
39. Han, S., Makareeva, E., Kuznetsova, N. V., DeRidder, A. M., Sutter, M. B., Losert, W., Phillips, C. L., Visse, R., Nagase, H., and Leikin, S. (2010) Molecular mechanism of type I collagen homotrimer resistance to mammalian collagenases. *J. Biol. Chem.* **285,** 22276–22281
40. Hinz, B. (2007) Formation and function of the myofibroblast during tissue repair. *J. Invest. Dermatol.* **127,** 526–537
41. Li, Y., Jiang, D., Liang, J., Meltzer, E. B., Gray, A., Miura, R., Wogensen, L., Yamaguchi, Y., and Noble, P. W. (2011) Severe lung fibrosis requires an invasive fibroblast phenotype regulated by hyaluronan and CD44. *J. Exp. Med.* **208,** 1459–1471
42. Wynn, T. A. (2011) Integrating mechanisms of pulmonary fibrosis. *J. Exp. Med.* **208,** 1339–1350
43. Strieter, R. M. (2008) What differentiates normal lung repair and fibrosis? Inflammation, resolution of repair, and fibrosis. *Proc. Am. Thorac. Soc.* **5,** 305–310
44. Madsen, D. H., Engelholm, L. H., Ingvarsen, S., Hillig, T., Wagenaar-Miller, R. A., Kjøller, L., Gårdsvoll, H., Høyer-Hansen, G., Holmbeck, K., Bugge, T. H., and Behrendt, N. (2007) Extracellular collagenases and the endocytic receptor, urokinase plasminogen activator receptor-associated protein/Endo180, cooperate in fibroblast-mediated collagen degradation. *J. Biol. Chem.* **282,** 27037–27045
45. Madsen, D. H., Ingvarsen, S., Jürgensen, H. J., Melander, M. C., Kjøller, L., Moyer, A., Honoré, C., Madsen, C. A., Garred, P., Burgdorf, S., Bugge, T. H., Behrendt, N., and Engelholm, L. H. (2011) The non-phagocytic route of collagen uptake: a distinct degradation pathway. *J. Biol. Chem.* **286,** 26996–27010
46. Madsen, D. H., Jürgensen, H. J., Ingvarsen, S., Melander, M. C., Vainer, B., Egerod, K. L., Hald, A., Rønø, B., Madsen, C. A., Bugge, T. H., Engelholm, L. H., and Behrendt, N. (2012) Endocytic collagen degradation: a novel mechanism involved in protection against liver fibrosis. *J. Pathol.* **227,** 94–105
47. Bundesmann, M. M., Wagner, T. E., Chow, Y. H., Altemeier, W. A., Steinbach, T., and Schnapp, L. M. (2012) Role of urokinase plasminogen activator receptor-associated protein in mouse lung. *Am. J. Respir. Cell Mol. Biol.* **46,** 233–239
48. Olson, A. L., Swigris, J. J., Lezotte, D. C., Norris, J. M., Wilson, C. G., and Brown, K. K. (2007) Mortality from pulmonary fibrosis increased in the United States from 1992 to 2003. *Am. J. Respir. Crit. Care. Med.* **176,** 277–284
49. Checa, M., Ruiz, V., Montaño, M., Velázquez-Cruz, R., Selman, M., and Pardo, A. (2008) MMP-1 polymorphisms and the risk of idiopathic pulmonary fibrosis. *Hum. Genet.* **124,** 465–472
50. Radisky, D. C., and Przybylo, J. A. (2008) Matrix metalloproteinase-induced fibrosis and malignancy in breast and lung. *Proc. Am. Thorac. Soc.* **5,** 316–322
51. Yang, K., Palm, J., König, J., Seeland, U., Rosenkranz, S., Feiden, W., Rübe, C., and Rübe, C. E. (2007) Matrix-metallo-proteinases and their tissue inhibitors in radiation-induced lung injury. *Int. J. Radiat Biol.* **83,** 665–676
52. Moraes, T. J., Chow, C. W., and Downey, G. P. (2003) Proteases and lung injury. *Crit. Care Med.* **31,** S189–S194
53. Richards, T. J., Kaminski, N., Baribaud, F., Flavin, S., Brodmerkel, C., Horowitz, D., Li, K., Choi, J., Vuga, L. J., Lindell, K. O., Klesen, M., Zhang, Y., and Gibson, K. F. (2012) Peripheral blood proteins predict mortality in idiopathic pulmonary fibrosis. *Am. J. Respir. Crit. Care Med.* **185,** 67–76
54. Chua, F., Dunsmore, S. E., Clingen, P. H., Mutsaers, S. E., Shapiro, S. D., Segal, A. W., Roes, J., and Laurent, G. J. (2007) Mice lacking neutrophil elastase are resistant to bleomycin-induced pulmonary fibrosis. *Am. J. Pathol.* **170,** 65–74
55. Taooka, Y., Maeda, A., Hiyama, K., Ishioka, S., and Yamakido, M. (1997) Effects of neutrophil elastase inhibitor on bleomycin-induced pulmonary fibrosis in mice. *Am. J. Respir. Crit. Care Med.* **156,** 260–265
56. Howell, D. C., Goldsack, N. R., Marshall, R. P., McAnulty, R. J., Starke, R., Purdy, G., Laurent, G. J., and Chambers, R. C. (2001) Direct thrombin inhibition reduces lung collagen, accumulation, and connective tissue growth factor mRNA levels in bleomycin-induced pulmonary fibrosis. *Am. J. Pathol* **159,** 1383–1395
57. Dabbagh, K., Chambers, R. C., and Laurent, G. J. (1998) From clot to collagen: coagulation peptides in interstitial lung disease. *Eur. Respir. J.* **11,** 1002–1005
58. Blanc-Brude, O. P., Archer, F., Leoni, P., Derian, C., Bolsover, S., Laurent, G. J., and Chambers, R. C. (2005) Factor Xa stimulates fibroblast procollagen production, proliferation, and calcium signaling via PAR1 activation. *Exp. Cell Res.* **304,** 16–27
59. Chambers, R. C., Dabbagh, K., McAnulty, R. J., Gray, A. J., Blanc-Brude, O. P., and Laurent, G. J. (1998) Thrombin stimulates fibroblast procollagen production via proteolytic activation of protease-activated receptor 1. *Biochem. J.* **333,** 121–127
60. Chambers, R. C., Leoni, P., Blanc-Brude, O. P., Wembridge, D. E., and Laurent, G. J. (2000) Thrombin is a potent inducer of connective tissue growth factor production via proteolytic activation of protease-activated receptor-1. *J. Biol. Chem.* **275,** 35584–35591
61. Yamaguchi, Y., Takihara, T., Chambers, R. A., Veraldi, K. L., Larregina, A. T., and Feghali-Bostwick, C. A. (2012) A peptide derived from endostatin ameliorates organ fibrosis. *Sci. Transl. Med.* **4,** 136ra171
62. Peretti, D., Bastide, A., Radford, H., Verity, N., Molloy, C., Martin, M. G., Moreno, J. A., Steinert, J. R., Smith, T., Dinsdale, D., Willis, A. E., and Mallucci, G. R. (2015) RBM3 mediates structural plasticity and protective effects of cooling in neurodegeneration. *Nature* **518,** 236–239
63. Liu, S. Q., Tefft, B. J., Roberts, D. T., Zhang, L. Q., Ren, Y., Li, Y. C., Huang, Y., Zhang, D., Phillips, H. R., and Wu, Y. H. (2012) Cardioprotective proteins upregulated in the liver in response to experimental myocardial ischemia. *Am. J. Physiol. Heart Circ. Physiol.* **303,** H1446–H1458
64. Shapiro, S. D. (1998) Matrix metalloproteinase degradation of extracellular matrix: biological consequences. *Curr. Opin. Cell Biol.* **10,** 602–608
65. Egeblad, M., and Werb, Z. (2002) New functions for the matrix metalloproteinases in cancer progression. *Nat. Rev. Cancer* **2,** 161–174
66. Visse, R., and Nagase, H. (2003) Matrix metalloproteinases and tissue inhibitors of metalloproteinases: structure, function, and biochemistry. *Circ. Res.* **92,** 827–839
67. Lee, H., Overall, C. M., McCulloch, C. A., and Sodek, J. (2006) A critical role for the membrane-type 1 matrix metalloproteinase in collagen phagocytosis. *Mol. Biol. Cell* **17,** 4812–4826
68. Everts, V., van der Zee, E., Creemers, L., and Beertsen, W. (1996) Phagocytosis and intracellular digestion of collagen, its role in turnover and remodelling. *Histochem. J.* **28,** 229–245
69. Lee, W., Sodek, J., and McCulloch, C. A. (1996) Role of integrins in regulation of collagen phagocytosis by human fibroblasts. *J. Cell. Physiol.* **168,** 695–704
70. Engelholm, L. H., List, K., Netzel-Arnett, S., Cukierman, E., Mitola, D. J., Aaronson, H., Kjøller, L., Larsen, J. K., Yamada, K. M., Strickland, D. K., Holmbeck, K., Danø, K., Birkedal-Hansen, H., Behrendt, N., and Bugge, T. H. (2003) uPARAP/Endo180 is essential for cellular uptake of collagen and promotes fibroblast collagen adhesion. *J. Cell Biol.* **160,** 1009–1015
71. Messaritou, G., East, L., Roghi, C., Isacke, C. M., and Yarwood, H. (2009) Membrane type-1 matrix metalloproteinase activity is regulated by the endocytic collagen receptor Endo180. *J. Cell Sci.* **122,** 4042–4048
72. Curino, A. C., Engelholm, L. H., Yamada, S. S., Holmbeck, K., Lund, L. R., Molinolo, A. A., Behrendt, N., Nielsen, B. S., and Bugge, T. H. (2005) Intracellular collagen degradation mediated by uPARAP/Endo180 is a major pathway of extracellular matrix turnover during malignancy. *J. Cell*

Biol. **169,** 977–985
73. Lee, T. H., McKleroy, W., Khalifeh-Soltani, A., Sakuma, S., Lazarev, S., Riento, K., Nishimura, S. L., Nichols, B. J., and Atabai, K. (2014) Functional genomic screen identifies novel mediators of collagen uptake. *Mol. Biol. Cell* **25,** 583–593
74. Riley, D. J., Berg, R. A., Soltys, R. A., Kerr, J. S., Guss, H. N., Curran, S. F., and Laskin, D. L. (1988) Neutrophil response following intratracheal instillation of collagen peptides into rat lungs. *Exp. Lung Res.* **14,** 549–563
75. Weathington, N. M., van Houwelingen, A. H., Noerager, B. D., Jackson, P. L., Kraneveld, A. D., Galin, F. S., Folkerts, G., Nijkamp, F. P., and Blalock, J. E. (2006) A novel peptide CXCR ligand derived from extracellular matrix degradation during airway inflammation. *Nat. Med.* **12,** 317–323